

# VizDefender: Unmasking Visualization Tampering through Proactive Localization and Intent Inference

Sicheng Song, Yanjie Zhang, Zixin Chen, Huamin Qu, Changbo Wang, and Chenhui Li

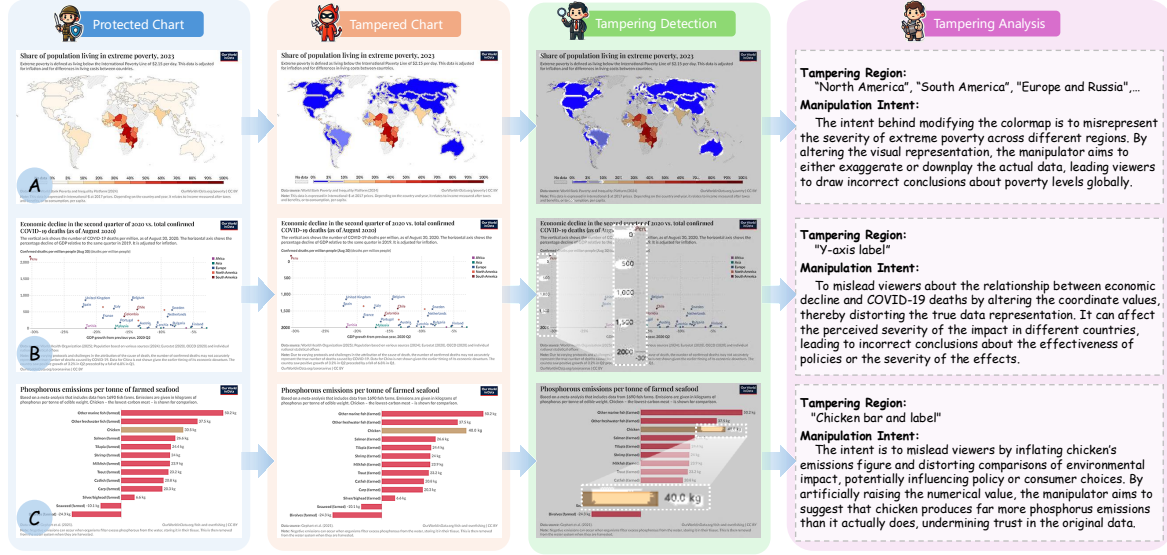


Fig. 1: This figure illustrates three different types of data tampering and their detection process. The Protected Visualization column shows the original visualizations with embedded location map: (A) Share of population living in extreme poverty in 2023 [22]; (B) Economic decline in the second quarter of 2020 vs. total confirmed COVID-19 deaths as of August 2020 [42]; (C) Phosphorous emissions per tonne of farmed seafood [51]. The Tampered Visualization column displays the tampered versions of these visualizations, which include modifying colormap, coordinate values, and data point values. The Tampering Detection column highlights the detected tampered areas using overlay masks. The Tampering Analysis column provides detailed explanations of each tampering region and its intent, revealing how the alterations mislead viewers and compromise the accuracy of the data.

**Abstract**— The integrity of data visualizations is increasingly threatened by image editing techniques that enable subtle yet deceptive tampering. Through a formative study, we define this challenge and categorize tampering techniques into two primary types: data manipulation and visual encoding manipulation. To address this, we present VizDefender, a framework for tampering detection and analysis. The framework integrates two core components: 1) a semi-fragile watermark module that protects the visualization by embedding a location map to images, which allows for the precise localization of tampered regions while preserving visual quality, and 2) an intent analysis module that leverages Multimodal Large Language Models (MLLMs) to interpret manipulation, inferring the attacker’s intent and misleading effects. Extensive evaluations and user studies demonstrate the effectiveness of our methods.

**Index Terms**—AI4VIS, Visualization Tampering Detection, Multimodal Large Language Model, Misinformation Visualization

## 1 INTRODUCTION

The integrity of data visualizations is crucial for informed decision-making. However, the digital age has brought an insidious threat: tampered visualizations. These are existing visualizations subtly manipulated—by altering original data or visual encodings—to distort the truth. This distinction is vital because tampered visualizations, by leveraging a authentic foundation, are more easily produced and disseminated than entirely fabricated visuals, and their “half-truth” nature makes them difficult to discern from genuine information.

- S. Song are both with East China Normal University and the Hong Kong University of Science and Technology E-mail: [csescsong@ust.hk](mailto:csescsong@ust.hk).
- Y. Zhang, Z. Chen, and H. Qu are with the Hong Kong University of Science and Technology E-mail: [yzhangvj, zchenf}@connect.ust.hk](mailto:{yzhangvj, zchenf}@connect.ust.hk), [huamin@ust.hk](mailto:huamin@ust.hk).
- C. Wang, C. Li are with the School of Computer Science and Technology, East China Normal University, E-mail: [chli, cbwang}@cs.ecnu.edu.cn](mailto:{chli, cbwang}@cs.ecnu.edu.cn).
- This work was supported by the National Natural Science Foundation of China under Grants 62572191 and 62472178, and by the Natural Science Foundation of Shanghai Municipality under Grant 24ZR1418300.
- Chenhui Li and Changbo Wang are the corresponding authors.

This poses a significant challenge for social media platforms, whose content moderation teams must protect users from widespread misinformation. As the World Economic Forum’s Global Risks Report 2025 highlights, misinformation and disinformation stand as the leading global concern in the near future, a top spot they have held for two years running [14]. Meanwhile, AI is also improving people’s critical thinking. Some empirical studies [4, 45] have confirmed that more and more people will use chatbots like Grok to check facts on social platforms such as Twitter. However, most of these fact checking tools are aimed at textual information and natural images. The ease with which image editing software and generative AI tools now enable such convincing alterations to existing visualizations has lowered the barrier for malicious actors. For social media content moderation teams who need to rapidly filter massive volumes of content and social media users who are often the producers and consumers of these visuals, manually assessing a single claim can take a professional several hours or days [50]. This urgent need for automated and precise detection for visual manipulation.

Watermarking is common on social media for copyright protection, but its application in visualization community has focused on data re-

trieval. Techniques like VisCode [70], InvVis [66], and VisGuard [65] embed robust watermarks (e.g., QR codes) that are designed to survive modifications to allow users to trace back to the original data. However, their robustness makes them unsuitable for precisely localizing tampered regions, which requires a semi-fragile signal. They also require complex workflows to store raw data and perform manual comparison. Meanwhile, general-purpose tampering detection networks [13, 62] and even proactive watermarking frameworks like EditGuard [72] are tailored for natural images and fail to address the unique structural properties of visualizations or infer manipulation intent.

To address these gaps and empower social media content moderation teams, we propose **VizDefender**, a framework for proactive tampering detection and intent analysis. Fig. 1 illustrates this entire workflow across three examples (A, B, C), walking through the full process from protection to analysis. Our framework consists of two main components. First, a semi-fragile watermark module leverages the fragility and locality properties of invertible neural networks (INNs) to embed a signal into the original *Protected Chart*. Semi-fragile watermarks are designed to tolerate benign operations like compression, but break predictably upon malicious edits to localize the tampered area. When a *Tampered Chart* is fed into our system, our method allows the module to precisely localize alterations (*Tampering Detection*) while remaining robust to benign changes like file compression. Second, an intent analysis and interpretation module (*Tampering Analysis*) uses a novel two-agent MLLM pipeline to semantically interpret these detected regions. This pipeline employs constrained, rule-based reasoning—mapping components like axes or bars to specific manipulation methods—to analyze the tamper, infer the manipulator’s intent, and explain its misleading effects. This constrained approach reduces model hallucination and improves interpretive accuracy. The deployment of such a proactive framework can help build a corpus of real-world tampering cases, paving the way for future data-driven passive detection models.

Our contributions include three aspects:

- (1) We conduct a formative interview study to reveal the definition and challenges of tampered visualizations and define a new problem of visualization tampering detection and analysis.
- (2) We introduce a novel framework for detecting and analyzing tampered visualizations using semi-fragile watermarking combined with intelligent interpretation leveraging MLLMs.
- (3) We validate the effectiveness of our framework through extensive quantitative evaluations against baseline methods and a user study.

## 2 RELATED WORK

Our work is situated at the intersection of three research areas. We first review how the visualization community has traditionally addressed misinformation, then examine existing image tampering detection techniques from computer vision, and finally discuss information steganography as the foundation for our proactive defense approach.

### 2.1 Misinformation Visualization

Misinformation in visualizations can distort public perception. Seminal works like Huff’s *How to Lie with Statistics* [28] and Tufte’s critique of “chart junk” [60] established a foundational understanding of how visual design choices can mislead.

Building on this, modern research has created extensive taxonomies of misleading design practices, such as truncating axes [11, 46] or creating deceptive visual encodings [32, 37]. To combat these issues, various automated tools and frameworks [9, 33, 43] have been developed to detect design flaws at the source code level. With the rise of reverse visualization engineering [49, 52], the pipelines of extracting raw data from bitmaps and pointing out design flaws or misleading areas has been implemented in many chart types such as bar charts [53], line charts [15], scatter plots [54], node-link diagrams [56–58], etc. In addition to these works, there are some studies focused on labeling potential misleaders [25] on graphs and strategies to explain common misleaders to the public [36].

However, these works focus on flaws introduced during the initial chart creation. It largely overlooks the growing threat of post-creation tampering, where a well-designed visualization is maliciously altered

at the image level. While recent studies have explored using MLLMs to identify misleading designs in chart images [10, 24, 38], detecting falsified data in a tampered static image remains a challenge. This specific gap motivates the need for dedicated tampering detection solutions.

### 2.2 Image Tampering Detection

While the visualization community has focused on design, the computer vision field has developed methods for image-level manipulation detection, though almost for natural images.

These methods can be broadly categorized as passive or proactive. Passive methods, such as ManTra-Net [62] and MVSS-Net [13], search for tampering artifacts without any prior information, but their performance depends heavily on the types of images and manipulations seen during training. Proactive methods, like MalP [3] and EditGuard [72], pre-emptively embed a digital watermark, to verify integrity of images.

Despite their sophistication, these techniques are not directly applicable to data visualizations. The subtle, semantic nature of chart tampering—where changing a few pixels can alter a data point’s value—is fundamentally different from the structural anomalies typically found in manipulated natural images. Existing models lack the semantic understanding of chart components, highlighting the need for a domain-specific proactive defense. This leads us to explore the specific application of information steganography in visualization images.

### 2.3 Information Steganography

Information Steganography is a technique used to embed hidden information into various types of carriers such as text, audio, video, and images. Among these carriers, images are the most widely used. Traditional methods mainly focus on the spatial domain [29, 44, 47] or the transformation domain [2, 59, 75]. With the development of deep learning, techniques such as autoencoders [5, 74] and GANs (Generative Adversarial Networks) [20] have been employed to optimize the embedding process, achieving better performance. Recently, Flow-based models have further advanced this field [16, 40, 67].

In visualizations, embedding metadata into visualization images has gained attention to maintain interactivity and integrity. For instance, Hota et al. [26] embedded digital watermarks into scientific visualizations to protect metadata, and Yang et al. [63] embedded watermarks in 3D models. For information visualization, this technique has been adopted for data integrity and retrieval. For example, systems like VisCode [70], Chartem [17], ChartStamp [18], InvVis [66], and VisGuard [65] embed information (e.g., QR codes linking to source data) into charts. The primary goal of these methods is data retrieval. Although they can be partially applied to tampering detection, they require additional costs to store and compare the original data, and trivial morphological comparison methods make it difficult for automated processes to accurately locate the tampering regions. Another gap is that these works do not use the semantic information of the visualizations to infer tampering.

Our work addresses this critical gap by developing an end-to-end framework for detecting and localizing tampering regions and infer manipulation intents in visualizations.

## 3 FORMATIVE INTERVIEW STUDY

We conducted a formative interview study to identify and categorize common tampering types performed on existing visualization images. The goal was to validate and refine the taxonomy of visual manipulation types [10, 32], ensuring that our research focuses on the most impactful and prevalent forms of manipulation.

**Participants:** Our study recruited 20 volunteers ( $\mu_{age} = 27.15$  years,  $STD_{age} = 6.54$ , 10 females and 10 males), most of whom were post-graduate students majoring data visualization, computer vision, or related fields. The interviewees also included two professors with over 10 years of experience in data visualization. All participants possessed foundational visualization literacy.

**Procedure:** We conducted semi-structured individual interviews online, each lasting approximately 30 minutes with additional time allowed if needed for participants to fully express their views. After obtaining informed consent, we presented the concepts of visualization

Table 1: Distribution of different visualization types in our training dataset.

Tampering Type	Potential Intent
Data Manipulation	Modifying Data Point Values (MDV) <i>Distort the true situation by exaggerating or downplaying specific data values.</i>
	Adding or Removing Data Points (ARD) <i>Alter trends or overall data distribution, influencing conclusions.</i>
	Modifying Coordinate Values (MCV) <i>Change the reference framework to mislead readers about the direction of trends.</i>
	Deceptive Auxiliary Annotations (DAA) <i>Guide readers toward specific, often incorrect, interpretations.</i>
	Modifying Legend (ML) <i>Alter legends to confuse readers about the categorization or significance of data.</i>
	Hiding Labels (HL) <i>Conceal important data labels to minimize their impact or obscure the true data.</i>
	Adding or Removing Logos (ARL) <i>Add or remove logos to mislead readers about the data's source or credibility.</i>
Visual Encoding Manipulation	Data-Visual Disproportion (DVD) <i>Modify visual elements to exaggerate or downplay the importance of data</i>
	Modifying Colormap (MC) <i>Change colors to mislead readers about data categories or distributions.</i>

Fig. 2: We summarized 9 identified common tampering types into two main categories based on their potential image manipulation intents. The bold letters are the abbreviations of each type.

tampering and misinformation. Participants were then asked to review an existing taxonomy [32] and a benchmark [10], providing feedback on which manipulation types could be achieved through image editing and suggesting new ones. The taxonomy offers a broad categorization of real-world misleading designs from a public perspective, while the benchmark provides a set of standardized D3-synthesized misleading chart examples, allowing our interview to be grounded in both in-the-wild flaws and controlled, systematic cases. The interviews focused on identifying visualization tampering, categorizing tampering types, their impact, and the challenges in their detection.

**Analysis:** We analyzed the interview data using thematic analysis [6], which yielded the following insights.

**Tampered visualizations are often more deceptive than traditional misleading visualizations.** Participants noted a difference in the perceived intention behind tampered visualizations compared to traditional misleading visualizations. While misleading visualizations may result from poor design choices or unintentional biases, tampered visualizations are deliberately altered to distort data and manipulate viewers' perceptions. Multiple participants (e.g., P1, P2, P6) remarked that tampered visualizations are specifically designed to deceive on purpose. As P1 stated, “*Tampered visualizations are designed to deceive on purpose. It's not just about poor design; it's a deliberate act to mislead.*” Participants also stated the relationship between tampered visualizations and misinformation visualizations. They observed that tampered visualizations are a significant subset of misinformation visualizations, including fake annotations, fake data, and biased interpretations. As P14 commented, “*Tampered visualizations are one part of the bigger picture of misinformation. They are insidious because they involve direct alterations to the visual elements, making it hard to trace the source of the manipulation.*” This insight was supported by several other participants (P7, P11), indicating the need to consider tampered visualizations within the diverse types of tampering.

**Detecting tampered visualizations is more challenging.** Participants highlighted that tampered visualizations, which are altered post-creation using image editing software, can be significantly more challenging to identify due to the subtlety of image differences. P3 noted, “*It's much harder to spot tampered visualizations because the changes are often very subtle and seamlessly integrated into the original image. You need to have a keen eye and a good understanding of data visualization to catch them.*” P8 echoed this sentiment, stating, “*Tampered charts can be very sophisticated. With advanced image editing software, it's possible to make changes that are nearly undetectable by human eyes.*” Participants also pointed out that image editing tools have become increasingly powerful and accessible, allowing non-experts to make convincing tampering to visualizations. This insight points to the need for techniques to detect tampered visualizations effectively.

**Understanding the manipulator's intent is crucial.** A crucial

Chart Type	Count	Chart Type	Count
graph	973	small multiple	303
scatterplot	860	matrix	272
heatmap	607	tree	241
bar chart	532	parallel coordinate	207
map	525	glyph-based	166
table	491	error bar	160
flow diagram	431	area chart	150
line chart	396	treemap	148
others	608		

insight from the interviews was the importance of understanding the intent behind the manipulation. Participants emphasized that the intent of the manipulator is a key factor that distinguishes visualization tampering from other forms of image types. P19 explained, “*The intent behind tampered visualizations is more diverse than those in natural images.*” This sentiment was echoed by P12, who stated, “*Understanding the intent behind the manipulation is crucial. It helps us identify the harmfulness of tampering and enhance the data literacy of the public.*” This insight highlights the need to focus on the manipulator's intent when developing strategies to detect and prevent tampered visualizations.

**Research scope of tampering types.** Through the interviews, several common tampering types were identified, which were categorized into two primary groups: data manipulation and visual encoding manipulation, which is as shown in Fig. 2. Data manipulation includes modifying data point values, adding or removing data points, and tampering coordinate values. For example, in bar charts, this involves modifying the values on bars to achieve wrong data insights. In line charts, this can modify the values on the coordinate axis to alter trends and data distribution. Modifying coordinate values can change the reference framework, leading readers to incorrect interpretations of data trends. These manipulations are intended to distort the actual situation by either exaggerating or downplaying specific data values, influencing conclusions drawn from the visualizations.

Visual encoding manipulation, on the other hand, involves deceptive auxiliary annotations, modifying legends, hiding labels, adding or removing logos, data-visual disproportion, and changing color maps. Deceptive auxiliary annotations can guide readers toward specific, often incorrect interpretations. In scatter plots, it can involve adding deceptive cluster circles to mislead perception of categories. Hiding labels can obscure important data, minimizing their impact. Adding or removing logos can mislead readers about the data's source or credibility. Data-visual disproportion involves altering visual elements. For instance, in bar charts, visual encoding manipulation might include changing the height of bars to exaggerate smaller values or altering the color map. Modifying color maps can mislead readers about data categories or distributions by changing colors or inverting color scales.

The refined taxonomy of visualization manipulation types will serve as a foundation for developing our intent inference model to address the challenges posed by tampered visualizations.

## 4 METHODS

Our framework as shown in Fig. 3 consists of two main components:

(1) *Semi-fragile Watermark Module:* The watermark processing stage includes both embedding and extraction models. Unlike traditional robust watermarks [65, 66] that aim to survive any transformation, our semi-fragile watermark is designed to be sensitive to image manipulations while remaining legitimate operations. The watermark is designed to maintain visual quality while ensuring detectability and spatial-related of various tampering operations. We also employed a posterior estimation [72] leverages prompts to strengthen watermark extraction under various degradations.

(2) *Intent Analysis and Interpretation:* The interpretation module leverages MLLMs to provide analysis of detected masks. This component processes both the tampering masks and visualization context to infer manipulation techniques and their potential misleading effects. The analysis helps users understand not just where tampering occurred, but also the intent behind the manipulation.

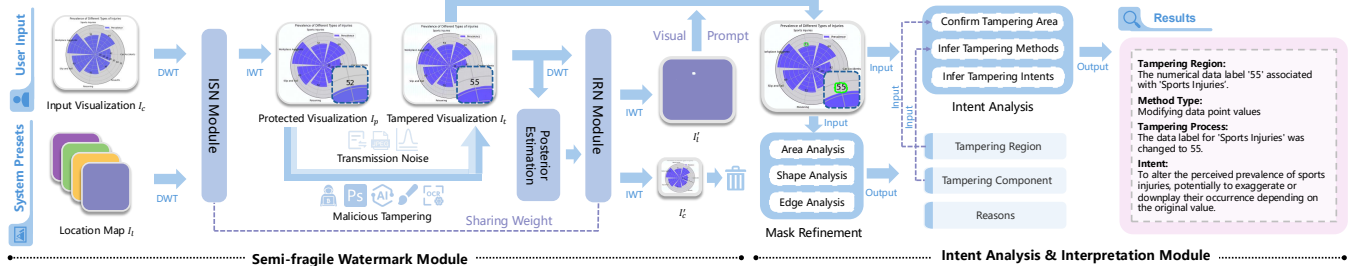


Fig. 3: Overview of VizDefender pipeline. Our framework consists of two components: Semi-fragile Watermark Module, and Intent Analysis & Interpretation. In the watermark processing stage, a flow-based model embeds the location map into the input visualization image, generating a protected visualization image that can be transmitted through networks. After potential tampering and transmission noise, an IRN module with posterior estimation extracts the watermark to generate the visual prompt on the tampered visualization. The intent analysis stage then processes both the tampered visualization with visual prompt through refinement and analysis modules, outputting intent results.

#### 4.1 Training Dataset

For training our semi-fragile watermark models, we curate a specialized dataset from VisImages [12], a visualization corpus containing 35,096 images from IEEE VIS publications. VisImages features expert-designed visualizations with diverse styles and complex layouts, making it suitable for training watermark-related models in visualization contexts. To ensure high-quality training data, we filter the original corpus based on image resolution, selecting only images with both height and width larger than 512 pixels. This filtering process results in 7,070 visualizations, which are then split into training (5,656 images, 80%) and validation (1,414 images, 20%) sets. The selected visualizations cover various types as shown in Table 1, ensuring our model's capability to handle different visualization types.

To accelerate convergence and enhance the robustness of our model, we initially pre-train it on the COCO dataset [34], which provides a diverse set of images and helps the model learn generalizable features. We used the Adam optimizer with an initial learning rate of  $1 \times 10^{-4}$ . For the pre-training phase, the model was trained for 250K iterations with a batch size of 4. Subsequently, for the fine-tuning phase on our curated VisImages dataset, we trained for an additional 10K iterations with an initial learning rate of  $1 \times 10^{-5}$  and a batch size of 4.

#### 4.2 Semi-fragile Watermark Module

Recent advances in image-to-image steganography using invertible neural networks (INNs) [39] have demonstrated impressive performance in information hiding. Through our observations, we discover two properties of INN-based steganography that make it suitable for tampering detection: (1) Fragility: when the container image undergoes tampering, the extracted watermark also exhibits damages, and (2) Locality: the damage to the extracted watermark precisely corresponds to the spatial location of the modifications, showing position-wise correlation.

Instead of trying to overcome these inherent characteristics as in previous works [65, 66], we leverage INN's natural fragility and locality for tampering detection. By designing a semi-fragile watermark that is sensitive to malicious manipulations while remaining stable under legitimate operations, we can localize tampered regions through comparing the extracted watermark with the original embedded one. When users input a clean visualization image  $I_c \in \mathbb{R}^{H \times W \times 3}$  into our system, along with a pre-defined location map  $I_l \in \mathbb{R}^{H \times W \times 3}$  (typically a solid-color image), our framework processes them through an ISN (Image Steganography Network) module. The ISN first applies DWT (Discrete Wavelet Transform) to decompose both  $I_c$  and  $I_l$  into frequency domains. Through invertible blocks, the network embeds  $I_l$  into  $I_c$  to generate a protected visualization  $I_p \in \mathbb{R}^{H \times W \times 3}$ . During network transmission,  $I_p$  may encounter various malicious manipulations and normal compressions, resulting in a tampered visualization  $I_t$ . The IRN (Image Revealing Network) module then processes  $I_t$  through invertible blocks and posterior estimation to extract the watermark  $I'_l$  and the reconstructed visualization  $I'_c$ . The damaged areas of  $I'_l$  are the area where the visualization is detected to be potentially tampered with.

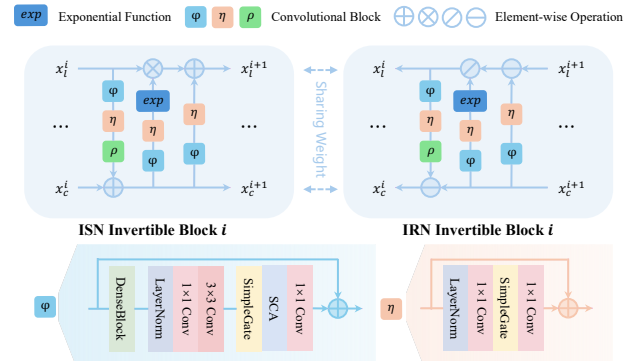


Fig. 4: The architecture of invertible blocks in ISN Module and IRN Module. Key components such as  $\phi$ ,  $\eta$ ,  $\exp$ , and  $\rho$  are integrated to enhance the transformation capabilities.

##### 4.2.1 Invertible Network

The key characteristic of INNs is that they allow reconstruction of inputs from their outputs through an inverse transformation. The core components of our INN are invertible blocks with affine coupling layers. These blocks follow a design pattern that ensures invertibility while maintaining expressive power: they split the input features into two parts and transform them alternately, with each part's transformation depending only on the other part. This design allows both forward and inverse computations to be tractable and computationally efficient.

To improve embedding quality and reduce visual artifacts, we first apply DWT to decompose both the input visualization  $I_c$  and location map  $I_l$  into frequency domains. The location map is a simple, pre-defined image (e.g., a checkerboard pattern) embedded as a fragile baseline. Any deviation in the extracted map directly reveals the spatial location of tampering. This frequency-domain decomposition helps our network concentrate watermark information in high-frequency components while preserving the visual structure in low-frequency components [21]. The transformed features then pass through a series of invertible blocks with affine coupling layers. For the  $i$ -th invertible block as shown in Fig. 4, the forward propagation of ISN is defined as:

$$\begin{aligned} x_l^{i+1} &= x_l^i \odot \exp(\eta(\phi(x_c^{i+1}))) + \eta(\phi(x_c^{i+1})) \\ x_c^{i+1} &= x_c^i + \rho(\eta(\phi(x_l^i))) \end{aligned} \quad (1)$$

where  $x_c^i$  and  $x_l^i$  represent the features of the visualization image and location map in the  $i$ -th layer respectively,  $\odot$  denotes element-wise multiplication, and  $\exp(\cdot)$  is the exponential function. The transformation functions  $\phi(\cdot)$  and  $\eta(\cdot)$  are implemented as a five-layer dense block [27] augmented with a lightweight feature interaction module [8]. In reverse, the revealing operation of IRN module can be computed as:

$$\begin{aligned} x_l^i &= (x_l^{i+1} - \eta(\phi(x_c^{i+1}))) \odot \exp(\eta(\phi(x_c^{i+1}))) \\ x_c^i &= x_c^{i+1} - \rho(\eta(\phi(x_l^i))) \end{aligned} \quad (2)$$

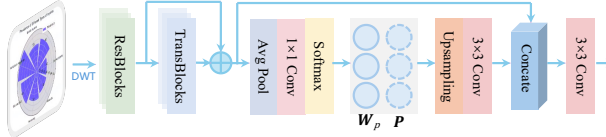


Fig. 5: The posterior estimation model.

#### 4.2.2 Posterior Estimation

To keep the semi-fragile watermark robust to some normal image degradations, we add a posterior estimation model [72] to IRN, which is shown to predict missing high-frequency information. The model (Fig. 5) helps our INNs to accurately recover the location map  $I_l$  from the tampered visualization  $I_t$ . The model first extracts local and non-local features  $F_t$  from the tampered visualization  $I_t$  using a combination of residual blocks and transformer blocks. This can be formulated as:

$$F_t = \zeta_2(\zeta_1(\text{DWT}(I_t))) + \zeta_1(\text{DWT}(I_t)) \quad (3)$$

where  $\zeta_1(\cdot)$  denotes 8 residual blocks [23] and  $\zeta_2(\cdot)$  denotes 4 transformer blocks [68]. Pre-defined degradation prompts  $P = [P_1, P_2, P_3]$  are learnable embedding tensors that represent three types of typical transmission noise including Gaussian Noise, JPEG, and Poisson Noise. These prompts are combined with the extracted features using dynamic weight coefficients  $W_p$  obtained via a average pooling layer, a  $1 \times 1$  convolution layer and a softmax operation. The fused features and degradation prompts generate the estimated posterior, which initializes the invertible blocks in the IRN, enabling accurate recovery of  $I_l$ .

#### 4.2.3 Loss Function

Our training objective is twofold: ensuring the visual fidelity of the protected visualization ( $I_p$ ) to the original ( $I_c$ ), and guaranteeing the accurate extraction of the location map ( $I_l$ ) from an untampered image. To achieve this, we define a total loss  $\mathcal{L}_{\text{total}}$  as a weighted sum of an encoding loss and an extraction loss. The encoding loss is the Mean Squared Error (MSE) between  $I_p$  and  $I_c$ , ensuring visual similarity. The extraction loss is the L1 loss between the original location map  $I_l$  and the extracted map  $I'_l$ , ensuring accurate recovery. The total loss function can be formulated as:

$$\mathcal{L}_{\text{total}} = \alpha \mathcal{L}_{\text{enc}} + \beta \mathcal{L}_{\text{ext}} = \alpha \mathcal{L}_{\text{mse}}(I_p, I_c) + \beta \mathcal{L}_{\text{L1}}(I'_l, I_l) \quad (4)$$

where  $\alpha$  and  $\beta$  are weighting coefficients.

The tampering mask  $M$  is obtained by comparing the residual between the predefined location map  $I_l$  and the reconstructed location map  $I'_l$ . We define the residual as:

$$M[i, j] = \theta_\tau(|I_l[i, j] - I'_l[i, j]|) \quad (5)$$

where  $\theta_\tau(x) = 1$  if  $x \geq \tau$ , otherwise 0. In our implementation, we set  $\tau$  to 0.2 based on our experience and observation.

### 4.3 Intent Analysis and Interpretation

The intent analysis and interpretation module is designed to interpret the manipulations identified by the watermark. This module leverages MLLMs to process detected tampering masks and infer the types of manipulations and their potential misleading effects.

To leverage the spatial reasoning capabilities of MLLMs while preserving chart context, we introduce a visual prompting mechanism. Instead of using a dense binary mask  $M$ , we first compute the connected components from the damaged location map. The boundary of these components are then overlaid as outlines on the tampered image. This serves as a visual prompt for the MLLM.

Our two-agent MLLM pipeline is designed to scaffold the user's analytical reasoning process based on bottom-up sensemaking process [48]. Specifically, our Component-to-Method Mapping rules (Fig. 7) are grounded in established visualization task taxonomies. These rules move the analysis beyond low-level pixel detection to a higher-level semantic inquiry [7]. The Mask Refinement Agent automates the low-level perceptual task of "anomaly identification," freeing the user's

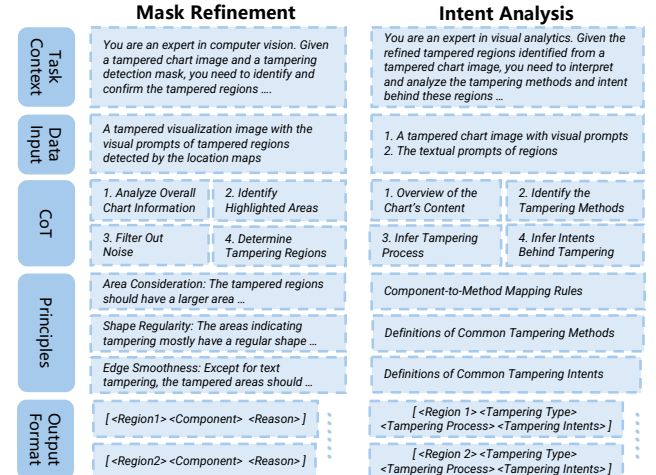


Fig. 6: Prompt structure of Intent Analysis and Interpretation Module.

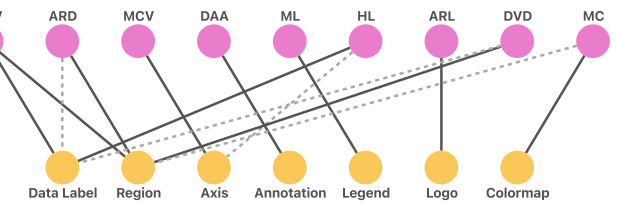


Fig. 7: The Component-to-Method mapping rules that guide the Intent Analysis Agent. Solid lines indicate a primary relationship (high likelihood), while dashed lines denote a secondary relationship. Tampering method abbreviations (top row) are defined in Fig. 2.

cognitive resources. The Intent Analysis Agent then addresses the higher-level analytical task of understanding why the anomaly exists. The prompt structure, as shown in Fig. 6, consists of five components. The complete prompts are available in the appendix.

#### 4.3.1 Mask Refinement Agent

The first agent, the Mask Refinement Agent, has two primary responsibilities. First, it refines the initial visual prompts to filter out noise. This is achieved by applying three analytical principles.

*Area Analysis:* It prioritizes larger bounding boxes corresponding to significant chart elements (e.g., data points, axes) while discarding small, isolated ones in blank spaces that are likely noise.

*Shape Analysis:* It favors regular shapes (rectangles, circles) that align with structured chart elements, helping to distinguish intentional tampering from random watermark damage of data transmission.

*Edge Analysis:* It checks for smooth, continuous edges in the highlighted regions, as irregular or jagged boundaries often indicate noise rather than a coherently manipulated element.

Second, the agent identifies the specific visualization component contained within each confirmed tampered region. Based on a predefined list, it categorizes each region as an *axis*, *data label*, *legend*, *colormap*, *region* (for data elements like bars or points), *logo*, or *annotation*. The output of this agent is a set of refined tampering regions paired with their corresponding component labels, which serves as a structured input for the next agent.

#### 4.3.2 Intent Analysis Agent

The Intent Analysis Agent is tasked with inferring the specific tampering method and the manipulator's underlying intent. To mitigate MLLM hallucination and ground its reasoning, this agent employs a constrained inference mechanism based on a predefined set of rules, as illustrated in Fig. 7. We defined these rules by mapping the tampering methods to the chart components they logically affect based on the existing misleading visualization gallery [32] and benchmark [10].

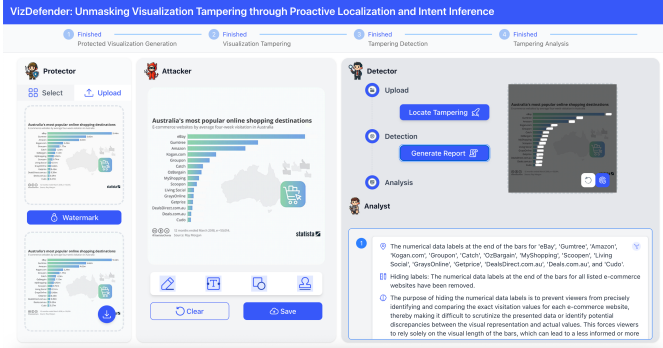


Fig. 8: The web-based interface of our VizDefender system, demonstrating the end-to-end workflow from proactive protection and simulated tampering to automated detection and intent analysis.

This mechanism works via a Component-to-Method Mapping. The component label provided by the first agent is used to query the rule set, which provides a prioritized list of likely tampering methods. For instance, if the identified component is a *data label*, the agent is instructed to first evaluate primary, high-likelihood methods such as “Modifying data point values” (MDV) or “Hiding labels” (HL). Only if these fail to explain the visual evidence will it consider secondary possibilities like “Adding or removing data points” (ARD).

The agent’s step-by-step reasoning process is as follows:

*Infer Tampering Method:* For each tampered region, the agent selects the most appropriate tampering method by following the Component-to-Method Mapping rules (Fig. 7). The taxonomy of methods is derived from our formative study (Fig. 2).

*Describe Tampering Process:* The agent provides a concise, one-sentence description of how the manipulation was likely performed.

*Infer Tampering Intent:* Finally, by analyzing the chosen method in the context of the overall visualization, the agent infers the potential motive behind the tampering.

## 5 APPLICATION

VizDefender is designed as a solution for social media platforms. To demonstrate the practical workflow of our framework, we developed an interactive system that embodies the entire proactive defense lifecycle, as shown in Fig. 8. The system guides different users through four key stages: (1) **Protector**: A content publisher uploads an original visualization. The social media platform watermarks the original visualization and outputs the protected visualization online. (2) **Attacker**: A hacker maliciously modifies the protected visualization and spreads the tampered visualization. (3) **Detector**: A content moderator of social media platform uploads the suspicious image to locate tampering. (4) **Analyst**: A fact-checker of social media platform or a curious user on social media reviews an automatically generated report detailing the manipulation and its inferred intent. This end-to-end process addresses the challenges of visual misinformation from two critical perspectives: scalable, platform-side content moderation and transparent, user-centric fact-checking.

### 5.1 Automated Content Moderation at Scale

Content moderation teams on social media platforms face an overwhelming, high-velocity stream of visual information, making manual review of every chart infeasible and leaving them vulnerable to sophisticated, large-scale misinformation campaigns. VizDefender addresses this critical need by functioning as an automated, platform-wide sentinel. Through a backend process of automatically watermarking all uploaded visualizations, it creates a fully verifiable ecosystem. This allows the platform’s integrity systems to scan millions of images at scale and instantly flag any tampered content, such as the chart with subtly inflated data points in Fig. 1(C). More importantly, this automated process moves platforms beyond simple, reactive moderation. By aggregating detection data—common topics, recurring manipulation methods, or coordinated timing—platforms can gain strategic

intelligence, identifying the macro-trends of disinformation and the potential organized efforts seeking to manipulate public discourse.

## 5.2 Empowering Users with Critical Thinking Tools

Beyond platform-level control, today’s social media users are increasingly seeking tools that empower their own critical thinking. For many, simply knowing a visualization is “fake” is insufficient; they are curious about the manipulator’s motive and want to understand *how* and *why* they are being misled. VizDefender directly meets this demand with a user-facing tool that emphasizes transparency and explanation. When a user activates the tool on a suspicious image, like the poverty map in Fig. 1(A). The system provides the evidence—the tampering mask revealing the manipulated colormap—and then addresses the crucial question of intent. The analysis module explains that the likely motive was to exaggerate the severity of poverty to evoke a stronger emotional response. This transforms a simple verification check into a learning moment, fostering a more discerning user base by revealing not just *what* was faked, but the narrative purpose behind the deception.

## 6 EVALUATION

We evaluate our method from three aspects: quality of protected visualization, accuracy of tampering detection, and accuracy of intent analysis. We conduct our experiments on a PC with a server with 4×NVIDIA RTX 3090. Our model is implemented with Pytorch. The weights (Equation 4) are set as  $\alpha = 100$  and  $\beta = 1$  to balance the image quality of protected visualization and location map decoding.

### 6.1 Test Dataset Composition

Our test dataset is comprised of two main components: a manually created dataset and an automatically generated dataset.

**Manually Created Dataset (MCD)** was developed by recruiting five volunteers who are proficient in various image editing technologies, and possess a background in visualization design. Each volunteer was tasked with modifying 20 visualizations according to nine distinct tampering types identified in our formative study (Fig. 2), as well as creating examples with a mixture subset including at least two methods. The collection results in a total of 100 visualizations. These volunteers were compensated at a rate of \$30 per hour for their time. The source visualizations for this dataset were sourced from Our World in Data [31] and InfoGraphicVQA [41], ensuring that there is no overlap with our training set. Volunteers were allowed to use any software they were familiar with to alter the visualization images. For each modified visualization, they saved a binary mask of the tampered regions as the ground truth. Additionally, they documented the tampering method and the intent behind each manipulation. To ensure the reliability of the data, two authors checked the dataset in a back-to-back manner.

**Automatically Generated Dataset (AGD)** was designed to evaluate the robustness of our method against various scales of tampering, without considering the intent behind the modifications. Due to the limitations of automated tampering methods, we focused on three primary tampering techniques that can be performed automatically: textual tampering, graphical element tampering, and painting.

• *Textual Tampering*: We employed OCR [55] to extract text from the visualizations and used GPT-4o-mini to infer the semantics of the extracted text within the context of the visualization. The original text was then replaced with synonyms or strings with similar parts of speech, using similar fonts and sizes, or was outright deleted.

• *Graphical Element Tampering*: Using the Segment Anything model [30], we segmented and filtered graphical elements within the visualization. We then performed random deletions, modifications, or copy-paste actions on these elements.

• *Painting*: Random circles, rectangles, and lines were added to the visualizations to simulate deceptive annotations.

The charts used for this dataset were sourced from the ChartQA-MLLM [69] dataset. For each tampering method, we created subsets with one, two, and three tampering instances per chart, resulting in 100 charts per subset. This process was repeated for each of the three tampering methods, creating a total of 9 subsets and 900 charts.

Table 2: The image quality evaluation results of protected visualizations

Method	MCD			AGD		
	P $\uparrow$	S $\uparrow$	L $\downarrow$	P $\uparrow$	S $\uparrow$	L $\downarrow$
EditGuard	32.57	0.85	0.0057	31.91	0.83	0.0114
<b>VizDefender</b>	<b>33.55</b>	<b>0.86</b>	<b>0.0028</b>	<b>33.49</b>	<b>0.85</b>	<b>0.0047</b>

Table 3: The evaluation results of tampering detection on MCD

Method	No Tampering		Post-Tampering	
	Noise Per. $\downarrow$	RMSE $\downarrow$	IoU $\uparrow$	F1 Score $\uparrow$
ManTraNet	2.41%	0.1466	0.0539	0.0870
MVSS-Net	4.14%	0.1628	0.0182	0.0462
EditGuard	0.45%	0.0624	0.5454	0.6669
<b>VizDefender</b>	<b>0.07%</b>	<b>0.0231</b>	<b>0.7272</b>	<b>0.8259</b>

## 6.2 Image Quality of Protected Visualization

The protected visualization is the visualization image with a semi-fragile watermark embedded into the input visualization through the encoding of localization maps. Our goal is to ensure that the protected visualization remains as visually similar to the original input visualization as possible. To evaluate the image quality of the protected visualization, we compare our method with the current state-of-the-art model for proactive defense against image tampering in natural images, EditGuard [72]. We use three metrics for this comparison: Peak Signal-to-Noise Ratio (PSNR) [1], Structural Similarity Index (SSIM) [61], and Learned Perceptual Image Patch Similarity (LPIPS) [71]. PSNR measures the ratio between the maximum possible signal power and the power of corrupting noise, with higher values indicating better quality. SSIM evaluates the visual quality by comparing structural information, luminance, and contrast, where values closer to 1 indicate higher similarity. LPIPS assesses perceptual similarity based on deep features, with lower values indicating better similarity.

The results in Table 2 show that VizDefender outperforms EditGuard across all metrics on both MCD and AGD datasets. VizDefender achieves higher PSNR and SSIM values, indicating better visual fidelity and structural similarity to the original visualizations, while its lower LPIPS score reflects superior perceptual similarity. The differences are statistically significant ( $p < 0.001$ ) based on a Paired Sample t-Test.

## 6.3 Accuracy of Tampering Detection

To evaluate tampering detection accuracy, we compare VizDefender with two passive techniques, ManTraNet [62] and MVSS-Net [13], and one proactive technique, EditGuard [72]. Our evaluation uses four metrics and covers two scenarios: reliability on untampered images and sensitivity on tampered images. For reliability, we measure Noise Percentage and Root Mean Square Error (RMSE). For sensitivity, we use Intersection over Union (IoU) and the F1 Score to assess the accuracy of the predicted tampering masks against the ground truth.

The results on the MCD, summarized in Table 3, demonstrate VizDefender’s effectiveness. On untampered images, VizDefender shows superior reliability with the lowest noise (0.07%) and RMSE (0.0231), indicating minimal false positives. On tampered images, it achieves the highest accuracy with an IoU of 0.7272 and an F1 Score of 0.8259. In contrast, the passive methods (ManTraNet, MVSS-Net) fail on this task, likely because they are designed for natural images. While EditGuard

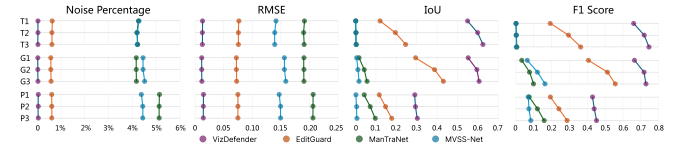


Fig. 10: The evaluation results of tampering detection on the AGD. The dataset tests the robustness of different methods against various scales of tampering through three primary techniques: Textual Tampering (T1, T2, T3), Graphical Element Tampering (G1, G2, G3), and Painting (P1, P2, P3). Each technique is evaluated over subsets with one, two, and three instances of tampering per visualization.

shows better generalization, it is still outperformed by our method, which is specifically tailored for visualizations.

This consistent superiority is further detailed in the per-category breakdown shown in Fig. 9. The radar charts visualize performance across ten tampering types. These correspond to the nine distinct manipulation methods defined in Fig. 2, plus a *MIX* category representing a combination of two or more methods. The results show that VizDefender establishes a dominant performance margin in every scenario. It maintains the lowest error rates and highest detection scores regardless of the manipulation methods, from subtle data point value changes (MDV) to complex colormap modifications (MC). This highlights the robustness and versatility of our method against a diverse range of real-world tampering strategies.

The evaluation on the AGD, shown in Fig. 10, further confirms VizDefender’s robustness. As the number of tampering instances increases (from 1 to 3), VizDefender maintains stable and high performance, while EditGuard’s accuracy degrades more significantly. The passive methods fail entirely. While challenging operations like painting fine lines affect all methods, VizDefender consistently delivers the most accurate results. A detailed metric values and error analysis are available in the supplementary materials.

## 6.4 Accuracy of Intent Inference

We evaluate our Intent Analysis and Interpretation module by comparing it with a straightforward prompt-based baseline. The latter involves directly feeding the tampered visualization and detected location maps into an MLLM without the assistance of two specific agents. Our evaluation is conducted on the MCD, utilizing Gemini-Flash-2.5 as the MLLM. We assess performance using the categorical accuracy of the inferred tampering method, and the semantic similarity of the inferred tampering process and intent. For semantic similarity, we extract text embeddings using the Gemini-Text-Embedding model and calculate the cosine similarity between our model’s outputs and the ground truth provided by the volunteers in our formative study.

First, we evaluate the model’s ability to correctly identify the tampering method. We use a strict evaluation criterion: a classification is only considered correct if the set of identified tampering types perfectly matches the ground truth set. Any additional, incorrect, or omitted types render the identification incorrect. As shown in Fig. 11, VizDefender achieves a total classification accuracy of **82%**, starkly outperforming the baseline’s 28%. This superiority is consistent across nearly all categories, and is particularly evident in cases like “Modifying Coordinate Values” (MCV) and “Adding or Removing Logos” (ARL), where VizDefender achieves 100% accuracy compared to the baseline’s 30% and 10%, respectively. This significant improvement in accuracy can be attributed to our structured Component-to-Method mapping, which constrains the MLLM’s reasoning and prevents it from making ungrounded classifications—a common failure mode for the unconstrained baseline.

Next, we assess the semantic quality of the generated explanations for the tampering process and intent. The results, visualized as distributions in Fig. 12, show that VizDefender’s outputs (blue) consistently achieve higher cosine similarity scores than the baseline (green) across almost all tampering types. On average, our method scores higher for both tampering process similarity (**0.874** vs. 0.836) and also for tampering intent similarity (**0.907** vs. 0.881). The tighter distributions

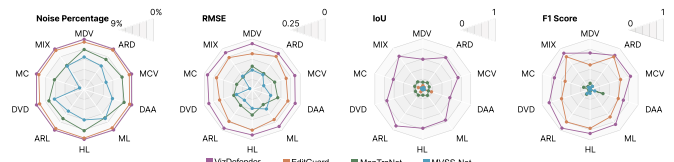


Fig. 9: Comparison of tampering detection methods on the MCD across different tampering types. For Noise Percentage and RMSE, lower values (closer to the edge) are better, while for IoU and F1 Score, higher values (closer to the edge) are better. VizDefender demonstrates superior performance over all baselines across all tampering types and metrics.

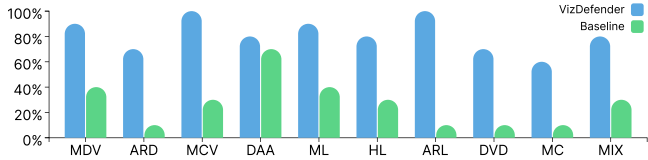


Fig. 11: The evaluation results of tampering method identification comparing with the baseline. The X-axis represents different tampering type, and the Y-axis represents the accuracy.

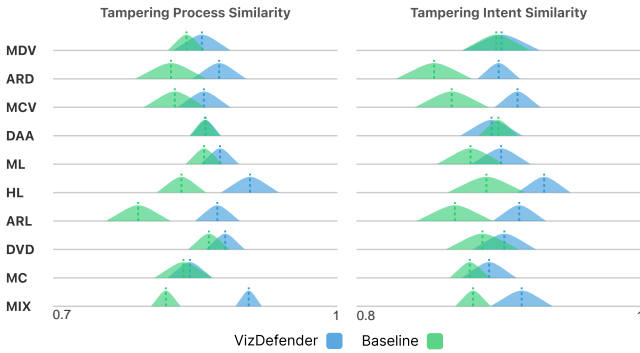


Fig. 12: The evaluation results of tampering process and intent. The central line of the mountain represents the mean values, and the two ends represent the 95% confidence interval.

for VizDefender also suggest a more stable and reliable performance.

The superior performance of our approach across both classification and semantic tasks is a direct result of our two-agent design. The Mask Refinement Agent provides clean and accurate spatial inputs, minimizing noise-induced errors. Subsequently, the Intent Analysis Agent, guided by its CoT framework and the crucial rule-based inference mechanism, drastically reduces model hallucination.

Some relatively lower score for tampering method analysis can be attributed to the absence of prior knowledge about the original visualization, which the ground truth inherently possesses. For manipulations such as deletions or modifications of text, logos, or numerical values, inferring the tampering method solely from the tampered image and mask is challenging. However, our method remains effective at intent inference because it focuses on the narrative and contextual clues provided by the visualization’s background story. More qualitative results and error analysis could be found in our supplementary materials.

## 7 USER STUDY

We designed a user study to evaluate VizDefender’s performance by a questionnaire. To ensure unbiased evaluation, all methods being compared were anonymized throughout the study, and the presentation order of different methods’ results was randomized for each participant. Participants were not informed which results corresponded to which methods until after completing the study. The study was conducted through a 7-point Likert Scale consisting of three sections:

(1) *Image Quality*: In this section, participants were presented with 5 sets of visualization images. Each set contained three versions of the same visualization: the original clean image, the image watermarked by VizDefender, and the image watermarked by EditGuard. Participants rated each image’s quality and readability.

(2) *Tampering Detection*: This section showed participants 5 sets of tampered visualizations. Each set included the original visualization image, the tampered image, and tampering detection results from four different methods: VizDefender, EditGuard, MVSS-Net, and ManTraNet. Participants evaluated the accuracy of each method’s detection mask.

(3) *Intent Inference*: The final section presented 5 tampering cases. For each case, participants were shown the tampered image with its detection mask, followed by two different tampering process and intent descriptions – one predicted by straightforward prompting and

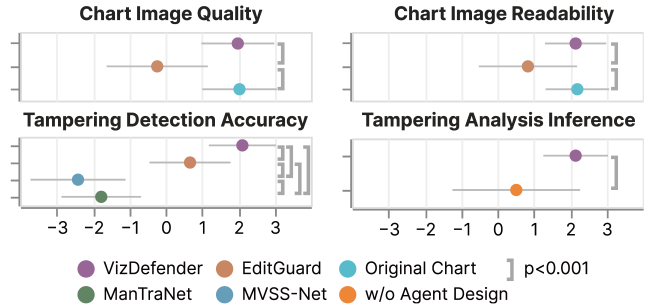


Fig. 13: The results of our user study. Each circle represents the mean score, with error bars indicating the standard deviation. The statistical significance, was assessed using the Wilcoxon signed-rank test.

another by VizDefender’s Intent Analysis module. Participants rated the reasonableness of each output.

Before starting the evaluation, participants were briefed about the general purpose of visualization tampering detection and analysis. They were then guided through a practice example to familiarize themselves with the rating tasks. The actual study took about 20 minutes.

**Participant:** We recruited 30 participants ( $\mu_{age} = 26.13$  years,  $STD_{age} = 2.70$ , 15 males and 15 females) by distributing the study in university academic groups. All participants were graduate students or researchers. Their self-reported academic backgrounds confirmed relevant expertise: 30 participants were from diverse related fields including Data Visualization/Analytics (9), Computer Vision (8), Human-Computer Interaction (5), and Computer Graphics (2), Design and Art (2), Education (2), Psychology (1), and Journalism and Literature (1).

**Analysis:** The results of our user study are as depicted in Fig. 13. Each evaluation metric in our user study was based on 150 samples, derived from 5 visualizations evaluated by 30 participants. The results indicate that our method excels in preserving image quality and readability, as users found it almost indistinguishable from the original visualizations. This highlights VizDefender’s ability to integrate protective measures without compromising visual integrity. In contrast, EditGuard’s watermarked images sometimes exhibited noticeable noise. This is likely due to the unique challenges posed by visualization images, which often contain large areas of blank space and continuous color blocks that are more susceptible to visual disruptions when watermarked. Our model, however, is specifically designed for visualization images, which enables it to manage these unique challenges while maintaining visual fidelity.

In the tampering detection phase, VizDefender demonstrated superior performance (2.113 vs. 0.673, -1.77, -2.41,  $p < 0.001$ ) by achieving a low false positive rate and exhibiting sensitivity to subtle visualization manipulations, such as color changes in legends. User feedback indicates that our method can more accurately display tampered areas without requiring manual comparison. This provides the first crucial piece of evidence for supporting user reasoning: by accurately and automatically localizing the manipulation, our framework automates the low-level perceptual task and directs the user’s attention.

In the intent inference analysis, VizDefender’s Intent Analysis module also demonstrated advantages over the straightforward prompt-based approach (2.15 vs. 0.52,  $p < 0.001$ ). This can be linked to the module’s utilization of agent-based techniques, which allows for a more nuanced understanding of the context and potential misleading effects of tampering. This proves how our framework supports a user’s ability to reason. While the detection mask answers *what* was changed, our module provides an answer for *why* it was changed. This high-level semantic interpretation moves beyond simple pixel-level detection and provides the user with the explicit context and motive needed to critically understand the impact of the manipulation, completing their reasoning process.

## 8 DISCUSSION

**Redefining Tampering: The Sanctity of Semantic Integrity.** Detecting tampering in visualizations is fundamentally different from in

natural images because visualizations are built on structured semantic encodings (e.g., axes, data points). We posit that this semantic integrity is paramount; therefore, any post-creation, image-level manipulation that alters the visual representation of data—even for seemingly benign rhetorical purposes—violates the original chart’s integrity and authorial intent. This stance creates a unique technical challenge: the system must differentiate between semantically-irrelevant benign changes (e.g., compression) and semantically-relevant manipulations (e.g., altering an axis value). Our evaluations showed that VizDefender’s domain-specific, semi-fragile approach is essential, as it is designed to protect not just pixels, but the semantic sanctity of the visualization. This highlights the necessity of specialized designs that protect not just pixels, but the semantic sanctity of the visualization.

**Rethinking Visual Prompts for MLLM-based Visualization Analysis.** A challenge we encountered was guiding the MLLM’s focus onto specific tampered regions within a chart. While visual prompting is a maturing area for natural images [35, 73], our findings reveal that its application to data visualizations is fraught with unique difficulties. Standard prompting techniques, such as spotlights, masks, or highlighting, proved problematic as they inherently alter the chart’s color encoding, thereby corrupting its original semantic meaning. For instance, a spotlight effect could mislead the MLLM into interpreting a bar’s color as a different data category. Alternative methods also proved inadequate. Bounding boxes lack the required precision for dense visualizations; a single box drawn around a segment of a line in a multi-line chart often ambiguously encompasses multiple data series. Annotations using text or arrows risk being confused with the chart’s native labels and graphical marks. Furthermore, we found that providing two separate images—one with and one without a visual prompt—led to poorer results. This suggests that current MLLMs possess weak spatial correspondence capabilities, and the alignment task between two images can introduce more hallucination and noise than it resolves.

Through trial-and-error, we used the contour lines of a tampered region’s connected components as the visual prompt. This reveals a divergence between human and machine perception. While humans find such outlines subtle and less intuitive than a spotlight, the MLLM responded to this precise, non-destructive prompt with the highest accuracy. This led to a hybrid design in VizDefender: we use these contour lines as the backend prompt for the MLLM, while rendering a more human-friendly spotlight effect in the user-facing interface. This discovery underscores a broader implication for the field. It suggests that interacting with MLLMs on visualizations [19, 64] may require a specialized visual language. Future research should focus on developing a dedicated visual prompting methodology for data visualizations—one that respects their semantic integrity and is tailored to the unique, and sometimes counter-intuitive, perceptual strengths of MLLMs, rather than simply adapting techniques designed for natural images.

**Trust in Visualizations Requires Proactive Defenses.** The ease with which visualization images can be tampered undermines public trust in data visualizations. The rapid dissemination of manipulated visual content on social media and other platforms underscores the limitations of reactive approaches to misinformation. Once tampered visualizations reach audiences, the damage to public perception is often irreversible, even if the manipulations are later exposed. Proactive defense systems address this challenge by embedding semi-fragile watermarks at the point of visualization creation, enabling tampering detection before manipulated visualizations can spread widely. Our proactive approach ensures that visualizations are protected from the outset, creating a layer of accountability for anyone attempting to manipulate them. Additionally, the integration of intent analysis allows stakeholders to assess the potential impact of tampering and respond accordingly. For social media platforms, our method provides an automated solution to identify and flag potentially manipulated visualizations during the content moderation process, helping prevent the viral spread of fake visualizations to maintain user trust.

**The Role of AI in Visual Misinformation: A Double-Edged Sword.** Our tools leverage AI to uncover subtle tampering and infer intent, empowering users to critically evaluate misinformation content. However, AI is also a double-edged sword: while it enables advanced

detection and analysis, generative AI technologies have lowered the barriers to creating convincing tampered visualizations, blurring the line between authentic and AI-generated content. The evolving landscape of AI-enabled misinformation emphasizes that technical solutions alone are insufficient. A comprehensive approach must combine technological defenses, with enhanced data literacy education to equip users with the skills to critically assess visualizations regardless of their source or creation method. This calls for a broader ecosystem of tools, policies, and educational initiatives to maintain trust in data visualization and safeguard its integrity in an era of rapidly advancing generative AI capabilities. As AI continues to evolve, the visualization community must adapt its strategies to preserve the trustworthiness of visual information and ensure its role as a reliable medium for communication.

**Limitation and Future Work.** The current version of VizDefender has several limitations in addressing visual misinformation detection and prevention. First, our system is unable to detect misinformation visualizations from scratch using generative AI tools. Such visualizations lack prior knowledge for comparison, posing a challenge for all existing tampering detection methods. Future work will explore statistical validation mechanisms to verify the consistency between raw data and its visual representation, as well as forensic techniques to identify inherent artifacts in AI-generated visualizations. Second, the reliance on semi-fragile watermarking introduces vulnerabilities under adversarial attacks targeting watermark integrity. We plan to explore adaptive watermarking techniques and complementary detection methods. Third, the time performance of MLLMs is a limitation for real-time applications. On our MCD, the Mask Refinement Agent required an average of 11.01s (95% CI: 10.57-11.45, T-test,  $p < 0.01$ ) and the Intent Analysis Agent required 11.04s (95% CI: 10.49-11.60, T-test,  $p < 0.01$ ). This latency presents a bottleneck for high-throughput moderation. Future work should explore optimization strategies, such as request parallelization and the use of smaller, specialized models.

Additionally, future directions include exploring interactive frameworks that allow users to steer the MLLM’s reasoning based on their own mental model, as our current module provides a one-shot explanation. Transforming the tool into a collaborative reasoning partner is a key next step, along with integrating proactive defenses into popular visualization platforms, exploring blockchain-based verification for authentic visualizations, and conducting user studies to refine system personalization. We also plan to expand training and evaluation to these “in-the-wild” visualizations (e.g., infographics, news media charts) found on social media.

## 9 CONCLUSION

In this paper, we addressed the critical challenge of malicious tampering in data visualizations, a growing threat to information integrity in the digital age. We introduced VizDefender, a proactive, end-to-end framework designed to not only detect manipulations but also to interpret their intent. Our approach combines a novel semi-fragile watermarking module for precise tampering localization with a sophisticated two-agent MLLM pipeline for intent analysis. This pipeline incorporates a constrained, rule-based reasoning mechanism that significantly reduces model hallucination and improves the accuracy of its interpretations.

Through extensive evaluations and user studies, we have demonstrated that VizDefender outperforms existing baselines in detection accuracy, visual quality, and the nuanced task of intent inference. Beyond its practical application as a tool for social media moderation, our work yields important insights for the broader AI and visualization communities. We acknowledge the limitations of our proactive approach, such as the inability to detect visualizations generated from scratch by AI and the inherent vulnerabilities of watermarking. Nonetheless, VizDefender represents a significant step toward safeguarding the trustworthiness of visual data. By providing a robust framework that bridges the gap between low-level pixel detection and high-level semantic interpretation, this work lays a critical foundation for future research in visualization security and helps ensure that data visualizations remain a reliable medium for communication.

## REFERENCES

- [1] A. Almohammad and G. Ghinea. Stego image quality and the reliability of psnr. In *2nd Intl. Conf. Image Process. Theory Tools Appl.*, pp. 215–220. IEEE, 2010. doi: [10.1109/ipta.2010.5586786](https://doi.org/10.1109/ipta.2010.5586786)
- [2] A. Almohammad, R. M. Hierons, and G. Ghinea. High capacity steganographic method based upon jpeg. In *Intl. Conf. Availability Reliability Security*, pp. 544–549. IEEE, 2008. doi: [10.1109/ares.2008.72](https://doi.org/10.1109/ares.2008.72)
- [3] V. Asnani, X. Yin, T. Hassner, and X. Liu. Malp: Manipulation localization using a proactive scheme. In *IEEE Conf. Comput. Vis. Pattern Recog.*, pp. 12343–12352, 2023. doi: [10.1109/cvpr52729.2023.01188](https://doi.org/10.1109/cvpr52729.2023.01188)
- [4] I. Augenstein, T. Baldwin, M. Cha, T. Chakraborty, G. L. Ciampaglia, D. Corney, R. DiResta, E. Ferrara, S. Hale, A. Halevy, et al. Factuality challenges in the era of large language models and opportunities for fact-checking. *Nature Machine Intelligence*, 6(8):852–863, 2024. 1
- [5] S. Baluja. Hiding images in plain sight: Deep steganography. *Adv. Neural Inform. Process. Syst.*, 30:1–11, 2017. doi: [10.23880/ijfsc-16000223](https://doi.org/10.23880/ijfsc-16000223)
- [6] V. Braun and V. Clarke. Using thematic analysis in psychology. *Qualitative research in psychology*, 3(2):77–101, 2006. doi: [10.1191/1478088706qp063oa](https://doi.org/10.1191/1478088706qp063oa) 3
- [7] M. Brehmer and T. Munzner. A multi-level typology of abstract visualization tasks. *IEEE Transactions on Visualization and Computer Graphics*, 19(12):2376–2385, 2013. doi: [10.1109/TVCG.2013.124](https://doi.org/10.1109/TVCG.2013.124)
- [8] L. Chen, X. Chu, X. Zhang, and J. Sun. Simple baselines for image restoration. In *Eur. Conf. Comput. Vis.*, pp. 17–33, 2022. doi: [10.1007/978-3-031-20071-7\\_2](https://doi.org/10.1007/978-3-031-20071-7_2)
- [9] Q. Chen, F. Sun, X. Xu, Z. Chen, J. Wang, and N. Cao. Vizlinter: A linter and fixer framework for data visualization. *IEEE Trans. Vis. Comput. Graph.*, 28(1):206–216, 2021. doi: [10.1109/tvcg.2021.3114804](https://doi.org/10.1109/tvcg.2021.3114804)
- [10] Z. Chen, S. Song, K. Shum, Y. Lin, R. Sheng, and H. Qu. Unmasking deceptive visuals: Benchmarking multimodal large language models on misleading chart question answering. *EMNLP*, pp. 1–31, 2025. doi: [10.48550/arXiv.2503.18172](https://doi.org/10.48550/arXiv.2503.18172) 2, 3, 5
- [11] M. Correll, E. Bertini, and S. Franconeri. Truncating the y-axis: Threat or menace? In *Proceedings of the 2020 CHI Conference on Human Factors in Computing Systems*, pp. 1–12, 2020. doi: [10.1145/3313831.3376222](https://doi.org/10.1145/3313831.3376222)
- [12] D. Deng, Y. Wu, X. Shu, J. Wu, S. Fu, W. Cui, and Y. Wu. Visimages: A fine-grained expert-annotated visualization dataset. *IEEE Trans. Vis. Comput. Graph.*, 29(7):3298–3311, 2023. doi: [10.1109/TVCG.2022.3155440](https://doi.org/10.1109/TVCG.2022.3155440) 4
- [13] C. Dong, X. Chen, R. Hu, J. Cao, and X. Li. Mvss-net: Multi-view multi-scale supervised networks for image manipulation detection. *IEEE Transactions on Pattern Analysis and Machine Intelligence*, 45(3):3539–3553, 2022. doi: [10.1109/tpami.2022.3180556](https://doi.org/10.1109/tpami.2022.3180556) 2, 7
- [14] M. Elsner, G. Atkinson, and S. Zahidi. The global risks report 2025, January 2025. Insight Report. 1
- [15] A. Fan, Y. Ma, M. Mancenido, and R. Maciejewski. Annotating line charts for addressing deception. In *Proceedings of the 2022 CHI Conference on Human Factors in Computing Systems*, pp. 1–12, 2022. doi: [10.1145/3491102.3502138](https://doi.org/10.1145/3491102.3502138) 2
- [16] H. Fang, Y. Qiu, K. Chen, J. Zhang, W. Zhang, and E.-C. Chang. Flow-based robust watermarking with invertible noise layer for black-box distortions. In *AAAI*, pp. 5054–5061, 2023. doi: [10.1609/aaai.v37i4.25633](https://doi.org/10.1609/aaai.v37i4.25633) 2
- [17] J. Fu, B. Zhu, W. Cui, S. Ge, Y. Wang, H. Zhang, H. Huang, Y. Tang, D. Zhang, and X. Ma. Chartem: reviving chart images with data embedding. *IEEE Trans. Vis. Comput. Graph.*, 27(2):337–346, 2020. doi: [10.1109/tvcg.2020.3030351](https://doi.org/10.1109/tvcg.2020.3030351) 2
- [18] J. Fu, B. Zhu, H. Zhang, Y. Zou, S. Ge, W. Cui, Y. Wang, D. Zhang, X. Ma, and H. Jin. Chartstamp: Robust chart embedding for real-world applications. In *ACM Int. Conf. Multimedia*, pp. 2786–2795, 2022. doi: [10.1145/3503161.3548286](https://doi.org/10.1145/3503161.3548286) 2
- [19] X. Fu, M. Liu, Z. Yang, J. R. Corring, Y. Lu, J. Yang, D. Roth, D. Florencio, and C. Zhang. Refocus: Visual editing as a chain of thought for structured image understanding. pp. 1–20, 2025. doi: [10.48550/arXiv.2501.05452](https://doi.org/10.48550/arXiv.2501.05452) 9
- [20] I. Goodfellow, J. Pouget-Abadie, M. Mirza, B. Xu, D. Warde-Farley, S. Ozair, A. Courville, and Y. Bengio. Generative adversarial nets. In *Adv. Neural Inform. Process. Syst.*, pp. 139–144, 2014. doi: [10.1145/3422622](https://doi.org/10.1145/3422622) 2
- [21] Z. Guan, J. Jing, X. Deng, M. Xu, L. Jiang, Z. Zhang, and Y. Li. Deepmih: Deep invertible network for multiple image hiding. *IEEE Trans. Pattern Anal. Mach. Intell.*, 45(1):372–390, 2022. doi: [10.1109/tpami.2022.3141725](https://doi.org/10.1109/tpami.2022.3141725) 4
- [22] J. Hasell, M. Roser, E. Ortiz-Ospina, and P. Arriagada. Poverty. *Our World in Data*, 2022. <https://ourworldindata.org/poverty>. 1
- [23] K. He, X. Zhang, S. Ren, and J. Sun. Deep residual learning for image recognition. In *IEEE Conf. Comput. Vis. Pattern Recog.*, pp. 770–778, 2016. doi: [10.1109/cvpr.2016.90](https://doi.org/10.1109/cvpr.2016.90) 5
- [24] J. Hong, C. Seto, A. Fan, and R. Maciejewski. Do llms have visualization literacy? an evaluation on modified visualizations to test generalization in data interpretation. *IEEE Trans. Vis. Comput. Graph.*, pp. 1–13, 2025. doi: [10.1109/TVCG.2025.3536358](https://doi.org/10.1109/TVCG.2025.3536358) 2
- [25] A. K. Hopkins, M. Correll, and A. Satyanarayan. Visualint: Sketchy in situ annotations of chart construction errors. In *Comput. Graph. Forum*, vol. 39, pp. 219–228. Wiley Online Library, 2020. doi: [10.1111/cgf.13975](https://doi.org/10.1111/cgf.13975) 2
- [26] A. Hota and J. Huang. Embedding meta information into visualizations. *IEEE Trans. Vis. Comput. Graph.*, 26(11):3189–3203, 2019. doi: [10.1109/tvcg.2019.2916092](https://doi.org/10.1109/tvcg.2019.2916092)
- [27] G. Huang, Z. Liu, L. Van Der Maaten, and K. Q. Weinberger. Densely connected convolutional networks. In *IEEE Conf. Comput. Vis. Pattern Recog.*, pp. 4700–4708, 2017. doi: [10.1109/cvpr.2017.243](https://doi.org/10.1109/cvpr.2017.243) 4
- [28] D. Huff. *How to lie with statistics*. WW Norton & Company, 1954. doi: [10.2307/2346789](https://doi.org/10.2307/2346789) 2
- [29] E. Kawaguchi and R. O. Eason. Principles and applications of bpcos steganography. In *Multimedia Syst. Appl.*, vol. 3528, pp. 464–473. SPIE, 1999. doi: [10.1117/12.337436](https://doi.org/10.1117/12.337436) 2
- [30] A. Kirillov, E. Mintun, N. Ravi, H. Mao, C. Rolland, L. Gustafson, T. Xiao, S. Whitehead, A. C. Berg, W.-Y. Lo, P. Dollar, and R. Girshick. Segment anything. In *Int. Conf. Comput. Vis.*, pp. 4015–4026, October 2023. doi: [10.1109/iccv51070.2023.00371](https://doi.org/10.1109/iccv51070.2023.00371) 6
- [31] G. C. D. Lab. Our world in data. <https://ourworldindata.org/>. 6
- [32] X. Lan and Y. Liu. “i came across a junk”: Understanding design flaws of data visualization from the public’s perspective. *IEEE Trans. Vis. Comput. Graph.*, 31(1):393–403, 2025. doi: [10.1109/TVCG.2024.3456341](https://doi.org/10.1109/TVCG.2024.3456341) 2, 3, 5
- [33] F. Lei, A. Fan, A. M. MacEachren, and R. Maciejewski. Geolinter: A linting framework for choropleth maps. *IEEE Trans. Vis. Comput. Graph.*, pp. 1592–1607, 2023. doi: [10.1109/tvcg.2023.3322372](https://doi.org/10.1109/tvcg.2023.3322372)
- [34] T.-Y. Lin, M. Maire, S. Belongie, J. Hays, P. Perona, D. Ramanan, P. Dollár, and C. L. Zitnick. Microsoft coco: Common objects in context. In *Eur. Conf. Comput. Vis.*, pp. 740–755, 2014. doi: [10.1007/978-3-319-10602](https://doi.org/10.1007/978-3-319-10602) -1\_48 4
- [35] W. Lin, X. Wei, R. An, P. Gao, B. Zou, Y. Luo, S. Huang, S. Zhang, and H. Li. Draw-and-understand: Leveraging visual prompts to enable llms to comprehend what you want. In *Int. Conf. Learn. Represent.*, pp. 1–30, 2025. doi: [10.48550/arXiv.2403.20271](https://doi.org/10.48550/arXiv.2403.20271) 9
- [36] L. Y.-H. Lo, Y. Cao, L. Yang, and H. Qu. Why change my design: Explaining poorly constructed visualization designs with explorable explanations. *IEEE Trans. Vis. Comput. Graph.*, pp. 955–964, 2023. doi: [10.1109/tvcg.2023.3327155](https://doi.org/10.1109/tvcg.2023.3327155) 2
- [37] L. Y.-H. Lo, A. Gupta, K. Shigyo, A. Wu, E. Bertini, and H. Qu. Misinformed by visualization: What do we learn from misinformative visualizations? In *Comput. Graph. Forum*, vol. 41, pp. 515–525. Wiley Online Library, 2022. doi: [10.1111/cgf.14559](https://doi.org/10.1111/cgf.14559) 2
- [38] L. Y.-H. Lo and H. Qu. How good (or bad) are llms at detecting misleading visualizations? *IEEE Trans. Vis. Comput. Graph.*, 31(1):1116–1125, 2025. doi: [10.1109/TVCG.2024.3456333](https://doi.org/10.1109/TVCG.2024.3456333) 2
- [39] S.-P. Lu, R. Wang, T. Zhong, and P. L. Rosin. Large-capacity image steganography based on invertible neural networks. In *IEEE Conf. Comput. Vis. Pattern Recog.*, pp. 10816–10825, 2021. doi: [10.1109/cvpr46437.2021.010674](https://doi.org/10.1109/cvpr46437.2021.010674)
- [40] R. Ma, M. Guo, Y. Hou, F. Yang, Y. Li, H. Jia, and X. Xie. Towards blind watermarking: Combining invertible and non-invertible mechanisms. In *ACM Int. Conf. Multimedia*, p. 1532–1542, 2022. doi: [10.1145/3503161.3547950](https://doi.org/10.1145/3503161.3547950) 2
- [41] M. Mathew, V. Bagal, R. Tito, D. Karatzas, E. Valveny, and C. Jawahar. Infographicvqa. In *Proceedings of the IEEE/CVF Winter Conference on Applications of Computer Vision (WACV)*, pp. 1697–1706, January 2022. doi: [10.1109/wacv51458.2022.00264](https://doi.org/10.1109/wacv51458.2022.00264) 6
- [42] E. Mathieu, H. Ritchie, L. Rodés-Guirao, C. Appel, D. Gavrilov, C. Giattino, J. Hasell, B. Macdonald, S. Dattani, D. Beltekian, E. Ortiz-Ospina, and M. Roser. Covid-19 pandemic. *Our World in Data*, 2020. <https://ourworldindata.org/coronavirus>. 1
- [43] A. McNutt and G. Kindlmann. Linting for visualization: Towards a practical automated visualization guidance system. In *VisGuides: 2nd Workshop on the Creation, Curation, Critique and Conditioning of Principles and*

- Guidelines in Visualization*, 2018. 2
- [44] J. Mielikainen. Lsb matching revisited. *IEEE Sign. Process. Letters*, 13(5):285–287, 2006. doi: 10.1109/lsp.2006.870357 2
- [45] I. Ortiz Del Noval and H. Y. Liew. Fact-checkers perception on social media governance models to combat disinformation: Insights from a european qualitative study. 2025. 1
- [46] A. V. Pandey, K. Rall, M. L. Satterthwaite, O. Nov, and E. Bertini. How deceptive are deceptive visualizations? an empirical analysis of common distortion techniques. In *Proceedings of the 2015 CHI Conference on Human Factors in Computing Systems*, pp. 1469–1478, 2015. doi: 10.1145/2702123.2702608 2
- [47] T. Pevný, T. Filler, and P. Bas. Using high-dimensional image models to perform highly undetectable steganography. In *Information Hiding, IH*, pp. 161–177. Springer, 2010. doi: 10.1007/978-3-642-16435-4\_13 2
- [48] P. Pirolli and S. Card. The sensemaking process and leverage points for analyst technology as identified through cognitive task analysis. In *Proceedings of international conference on intelligence analysis*, vol. 5, pp. 2–4. McLean, VA, USA, 2005. 5
- [49] J. Poco and J. Heer. Reverse-engineering visualizations: Recovering visual encodings from chart images. In *Comput. Graph. Forum*, vol. 36, pp. 353–363. Wiley Online Library, 2017. doi: 10.1111/cgf.13193 2
- [50] D. Quelle and A. Bovet. The perils and promises of fact-checking with large language models. *Frontiers in Artificial Intelligence*, 7:1341697, 2024. 1
- [51] H. Ritchie and M. Roser. Fish and overfishing. *Our World in Data*, 2021. <https://ourworldindata.org/fish-and-overfishing>. 1
- [52] M. Savva, N. Kong, A. Chhajta, L. Fei-Fei, M. Agrawala, and J. Heer. Revision: Automated classification, analysis and redesign of chart images. In *Proceedings of the 24th annual ACM symposium on User interface software and technology*, pp. 393–402, 2011. doi: 10.1145/2047196.2047247 2
- [53] A. Schlieder, J. Rummel, P. Albers, and F. Sadlo. The role of metacognition in understanding deceptive bar charts. In *2024 IEEE Workshop on Evaluation and Beyond - Methodological Approaches to Visualization (BELIV)*, pp. 51–59, 2024. doi: 10.1109/beliv64461.2024.00011 2
- [54] D. Shi, A. Oulasvirta, T. Weintrauf, and N. Cao. Understanding and automating graphical annotations on animated scatterplots. In *2024 IEEE 17th Pacific Visualization Conference (PacificVis)*, pp. 212–221, 2024. doi: 10.1109/PacificVis60374.2024.00031 2
- [55] R. Smith. An overview of the tesseract ocr engine. In *Ninth International Conference on Document Analysis and Recognition (ICDAR 2007)*, vol. 2, pp. 629–633, 2007. doi: 10.1109/ICDAR.2007.4376991 6
- [56] S. Song, C. Li, D. Li, J. Chen, and C. Wang. Graphdecoder: Recovering diverse network graphs from visualization images via attention-aware learning. *IEEE Trans. Vis. Comput. Graph.*, pp. 3074–3088, 2022. doi: 10.1109/tvcg.2022.3225554 2
- [57] S. Song, C. Li, Y. Sun, and C. Wang. Vividgraph: Learning to extract and redesign network graphs from visualization images. *IEEE Transactions on Visualization and Computer Graphics*, 29(7):3169–3181, 2023. doi: 10.1109/TVCG.2022.3153514 2
- [58] S. Song, Y. Zhang, Y. Lin, H. Qu, C. Wang, and C. Li. Gvvst: Image-driven style extraction from graph visualizations for visual style transfer. *IEEE Transactions on Visualization and Computer Graphics*, pp. 1–16, 2024. doi: 10.1109/TVCG.2024.3485701 2
- [59] M. D. Swanson, B. Zhu, B. Chau, and A. H. Tewfik. Multiresolution video watermarking using perceptual models and scene segmentation. In *IEEE Int. Conf. Image Process.*, vol. 2, pp. 558–561. IEEE, 1997. doi: 10.1109/icip.1997.638832 2
- [60] E. R. Tufte and P. R. Graves-Morris. *The visual display of quantitative information*. Graphics press Cheshire, CT, 1983. doi: 10.1016/0266-9838(86)90040-7 2
- [61] Z. Wang, A. C. Bovik, H. R. Sheikh, and E. P. Simoncelli. Image quality assessment: from error visibility to structural similarity. *IEEE Trans. Image Process.*, pp. 600–612, 2004. doi: 10.1109/tip.2003.819861 7
- [62] Y. Wu, W. AbdAlmageed, and P. Natarajan. Mantra-net: Manipulation tracing network for detection and localization of image forgeries with anomalous features. In *IEEE Conf. Comput. Vis. Pattern Recog.*, pp. 9535–9544, 2019. doi: 10.1109/cvpr.2019.00977 2, 7
- [63] J. Yang, D. Ruan, J. Huang, X. Kang, and Y.-Q. Shi. An embedding cost learning framework using gan. *IEEE Transactions on Information Forensics and Security (TIFS)*, pp. 839–851, 2019. doi: 10.1109/tifs.2019.2922229 2
- [64] X. Yang, Y. Wu, Y. Zhu, N. Tang, and Y. Luo. Askchart: Universal chart understanding through textual enhancement. *arXiv preprint arXiv:2412.19146*, 2024. doi: 10.48550/arXiv.2412.19146 9
- [65] H. Ye, J. Chen, S. Zhang, Y. Zhang, C. Wang, and C. Li. Visguard: Securing visualization dissemination through tamper-resistant data retrieval. *IEEE Trans. Vis. Comput. Graph.*, 2026. doi: 10.48550/arXiv.2507.14459 2, 3, 4
- [66] H. Ye, C. Li, Y. Li, and C. Wang. Invvis: Large-scale data embedding for invertible visualization. *IEEE Trans. Vis. Comput. Graph.*, 30(1):1139–1149, 2024. doi: 10.1109/TVCG.2023.3326597 2, 3, 4
- [67] H. Ye, S. Zhang, S. Jiang, J. Liao, S. Gu, C. Wang, and C. Li. Pprsteg: Printing and photography robust qr code steganography via attention flow-based model. *arXiv preprint arXiv:2405.16414*, pp. 1–8, 2024. doi: 10.48550/arXiv.2405.16414 2
- [68] S. W. Zamir, A. Arora, S. Khan, M. Hayat, F. S. Khan, and M.-H. Yang. Restormer: Efficient transformer for high-resolution image restoration. In *IEEE Conf. Comput. Vis. Pattern Recog.*, pp. 5718–5729, 2022. doi: 10.1109/cvpr52688.2022.00564 5
- [69] X. Zeng, H. Lin, Y. Ye, and W. Zeng. Advancing multimodal large language models in chart question answering with visualization-referenced instruction tuning. *IEEE Trans. Vis. Comput. Graph.*, 31(1):525–535, 2025. doi: 10.1109/TVCG.2024.3456159 6
- [70] P. Zhang, C. Li, and C. Wang. Viscode: Embedding information in visualization images using encoder-decoder network. *IEEE Trans. Vis. Comput. Graph.*, 27(2):326–336, 2020. doi: 10.1109/tvcg.2020.3030343 2
- [71] R. Zhang, P. Isola, A. A. Efros, E. Shechtman, and O. Wang. The unreasonable effectiveness of deep features as a perceptual metric. In *IEEE Conf. Comput. Vis. Pattern Recog.*, pp. 586–595, 2018. doi: 10.1109/cvpr.2018.00068 7
- [72] X. Zhang, R. Li, J. Yu, Y. Xu, W. Li, and J. Zhang. Editguard: Versatile image watermarking for tamper localization and copyright protection. In *IEEE Conf. Comput. Vis. Pattern Recog.*, pp. 11964–11974, 2024. doi: 10.1109/cvpr52733.2024.01137 2, 3, 5, 7
- [73] Y. Zhang, S. Qian, B. Peng, S. Liu, and J. Jia. Prompt highlighter: Interactive control for multi-modal llms. In *IEEE Conf. Comput. Vis. Pattern Recog.*, pp. 13215–13224, 2024. doi: 10.1109/cvpr52733.2024.01255 9
- [74] J. Zhu, R. Kaplan, J. Johnson, and L. Fei-Fei. Hidden: Hiding data with deep networks. In *Eur. Conf. Comput. Vis.*, pp. 657–672, 2018. doi: 10.1007/978-3-030-01267-0\_40 2
- [75] W. Zhu, Z. Xiong, and Y.-Q. Zhang. Multiresolution watermarking for images and video. *IEEE Trans. Circuit Syst. Video Technol.*, 9(4):545–550, 1999. doi: 10.1109/76.767121 2

## A PROMPT TEMPLATES

The following are the prompts for the mask refinement agent and the intent analysis agent in the intent analysis and interpretation module.

### Mask Refinement Agent

#### Task Context

You are an expert in computer vision. Given a tampered chart image, and we have detected the tampered areas and marked them with green lines.

You should provide the refined tampered regions and components as output, considering the principles provided.

The components to consider are:

- axis
- data labels
- legend
- colormap
- region
- logo
- annotation

#### Data Input

Tampered Visualization Image with Visual Prmopt: `{chart_img_path}`

#### Chain-of-Thought

Your reasoning should retain only confirmed information. Here is a potential checklist for inferring the tampering area:

1. Analyze the overall information conveyed by the visualization.
2. Identify the areas surrounded by green lines, which indicate potential tampering regions.
3. Filter out noise from the highlighted areas and determine where meaningful tampering has actually occurred.
3. Determine the tampering regions and corresponding components.

#### Principles

To filter out noise, you may refer to the three principles:

- **Area Analysis:** Prioritize highlighting sufficiently large areas and filter out minor areas along the background or edges that are likely noise. When you find a very small highlighted area on a relatively large color block, shape, or text, it is highly likely to be noise.
- **Shape Analysis:** For highlighted visual elements, focus on regular shapes (e.g., rectangles or circles) to detect potential tampering and disregard irregular shapes that suggest noise.
- **Edge Analysis:** Except for text modifications, the highlighted tampered areas should have smooth edges and fully cover the manipulated regions.

#### Output Format

Return the output in this strict format:

```
'''json
{
  "tampered_regions": [
    {
      "tampered_region": "<tampered region>",
      "tampered_component": ["<tampered component 1>", "<tampered component 2>", ...]
      "reason": "reason for tampered region"
    },
    ...
  ]
},
```

## Intent Analysis Agent

### Task Context

You are an expert in visual analytics. Given the refined tampered regions identified from a tampered visualization image, you need to interpret and analyze the tampering intent behind these regions.

You should provide a detailed analysis of the tampering intent, including the types of manipulations and their potential misleading effects.

### Data Input

Tampered Visualization Image with Visual Prompt: {chart\_img\_path}

Textual Prompt of Tampered Region: {tampered\_region\_json\_path}

### Component-to-Method Mapping Rules

For a given tampering\_component, you must evaluate the Primary Methods first. Only if none of the primary methods accurately describe the manipulation should you consider the Secondary Methods.

- If tampering\_component is "region":
  - Primary Methods: Modifying data point values, Adding or removing data points, Data-visual disproportion
  - Secondary Methods: Modifying the colormap
- If tampering\_component is "data labels":
  - Primary Methods: Modifying data point values, Hiding labels
  - Secondary Methods: Adding or removing data points, Data-visual disproportion
- If tampering\_component is "axis":
  - Primary Methods: Modifying coordinate values
  - Secondary Methods: Hiding labels
- If tampering\_component is "legend":
  - Primary Method: Modifying the legend
- If tampering\_component is "annotation":
  - Primary Method: Deceptive auxiliary annotations
- If tampering\_component is "logo":
  - Primary Method: Adding or removing logos
- If tampering\_component is "colormap":
  - Primary Method: Modifying the colormap

### Chain-of-Thought

Let's think step by step about the tampering intent. Here is a potential checklist for inferring the tampering intent:

1. Understand the context and a full understanding of the input
2. For each tampered region, first identify its tampering\_component from the input. Then, using the **Component-to-Method Mapping Rules** above, select the most fitting method. Remember to check Primary Methods before Secondary ones.
3. Based on your analysis, provide a simple description of the tampering process (tamper) in one sentence — how the original image was tampered to become the current version. For example: "Increase the population value of England from 53 million to 60 million and decrease the population value of Scotland from 5.2 million to 4 million.", "Remove the data points for feeling hopeful about the future"
4. Infer the intent based on the primary message conveyed by the chart and the identified tampered areas.

### Principles

To infer the tampering intents, you may refer to these common tampering types:

- **Modifying data point values:** Changing the quantitative value of an existing data point, which alters its visual representation (e.g., making a bar taller/shorter, moving a point up/down, changing the height of a line segment, or altering the boundary of an area). Crucially, in this method, the visual element is consistently updated to accurately reflect the new (modified) data point value. The visual element representing the data point remains present on the chart, but its specific value has been changed.
- **Adding or removing data points:** Introducing entirely new data points (and their corresponding visual elements) or completely deleting existing data points (and their corresponding visual elements). This results in visual elements appearing or disappearing from the chart, rather than just changing their existing properties.
- **Modifying coordinate values:** Changing the values or textual labels of x-axis or y-axis to alter their position in the chart.
- **Deceptive auxiliary annotations:** Using misleading annotations (e.g., clustering boxes, guide lines, arrows) to create a false impression.
- **Modifying the legend:** Changing the legend's content, colors, or order to mislead viewers about what the data represents.
- **Hiding labels:** Removing data labels near data points (e.g., scatter, point, etc.) to obscure the true meaning of the data.
- **Adding or removing logos:** Inserting or deleting logos to mislead viewers about the data source.
- **Data-visual disproportion:** Making the visual representation of data inconsistent with the actual values. This occurs when the visual element (e.g., bar length, area size) does not accurately correspond to its stated numerical value, or when one is modified without the other being consistently updated, creating a mismatch.
- **Modifying the colormap:** Adjusting the color mapping (including legend, data points, and their background colors) to distort the perception of data distribution, or introducing inconsistent colors to mislead.
- **Others:** Any other tampering method that is not included in the above types.

### Output Format

Return in JSON format with the following structure:

```
  {"json":  
  { "tampering_intents": [  
    {  
      "tampered_region": "<tampered region>",  
      "method": "<Tampering Method>",  
      "tamper": "<Tampering Process>",  
      "intent": "<Tampering Intent>"  
    },...]  
  },...}
```

## B QUANTITATIVE EVALUATION RESULTS

### B.1 Image Quality of Protected Visualization

Table 4: The image quality evaluation results of protected visualizations on the MCD. The Mean column represents the average value of each metric (SSIM, PSNR, LPIPS). The Lower and Upper columns indicate the 95% confidence interval for each metric.

Method	Subset	SSIM ↑			PSNR ↑			LPIPS ↓		
		Mean	Lower	Upper	Mean	Lower	Upper	Mean	Lower	Upper
VizDefender	Modifying Data Point Values	0.8576	0.8436	0.8716	33.5409	33.2815	33.8003	0.0030	0.0022	0.0039
	Adding or Removing Data Points	0.8582	0.8441	0.8722	33.2812	32.8249	33.7374	0.0023	0.0018	0.0028
	Modifying Coordinate Values	0.8587	0.8515	0.8658	33.4550	33.3407	33.5692	0.0032	0.0027	0.0037
	Deceptive Auxiliary Annotations	0.8557	0.8485	0.8628	33.6791	33.4246	33.9337	0.0032	0.0024	0.0040
	Modifying Legend	0.8575	0.8487	0.8662	33.3777	33.1043	33.6512	0.0031	0.0026	0.0037
	Hiding Labels	0.8565	0.8344	0.8785	33.6103	33.0719	34.1488	0.0028	0.0023	0.0032
	Adding or Removing Logos	0.8515	0.8377	0.8654	33.5891	33.1479	34.0303	0.0027	0.0022	0.0032
	Data-Visual Disproportion	0.8857	0.8752	0.8961	34.0616	33.8462	34.2770	0.0018	0.0016	0.0020
	Modifying Colormap	0.8620	0.8446	0.8794	33.5988	33.2944	33.9031	0.0026	0.0020	0.0031
	Mixture	0.8633	0.8520	0.8745	33.3248	32.6344	34.0152	0.0028	0.0022	0.0034
EditGuard	Modifying Data Point Values	0.8474	0.8327	0.8621	32.3916	31.4849	33.2983	0.0067	0.0047	0.0088
	Adding or Removing Data Points	0.8517	0.8366	0.8668	32.4421	31.9697	32.9144	0.0043	0.0032	0.0054
	Modifying Coordinate Values	0.8461	0.8358	0.8564	32.5298	32.1043	32.9553	0.0057	0.0046	0.0068
	Deceptive Auxiliary Annotations	0.8427	0.8289	0.8566	33.0031	32.6574	33.3488	0.0057	0.0046	0.0069
	Modifying Legend	0.8483	0.8354	0.8612	32.7114	32.3867	33.0361	0.0057	0.0046	0.0067
	Hiding Labels	0.8482	0.8243	0.8721	32.4081	31.8434	32.9728	0.0057	0.0047	0.0067
	Adding or Removing Logos	0.8461	0.8329	0.8593	32.8864	32.3671	33.4056	0.0053	0.0036	0.0070
	Data-Visual Disproportion	0.8776	0.8667	0.8884	32.8792	32.5107	33.2477	0.0051	0.0039	0.0063
	Modifying Colormap	0.8550	0.8372	0.8727	32.4965	31.9868	33.0063	0.0063	0.0037	0.0089
	Mixture	0.8550	0.8441	0.8658	31.9244	30.7683	33.0805	0.0069	0.0042	0.0095

Table 5: The image quality evaluation results of protected visualizations on the AGD. The Mean column represents the average value of each metric (SSIM, PSNR, LPIPS). The Lower and Upper columns indicate the 95% confidence interval for each metric.

Method	Subset	SSIM ↑			PSNR ↑			LPIPS ↓		
		Mean	Lower	Upper	Mean	Lower	Upper	Mean	Lower	Upper
VizDefender	Textual Tampering - 1	0.8513	0.8476	0.8549	33.4918	33.2611	33.7225	0.0046	0.0040	0.0052
	Textual Tampering - 2	0.8511	0.8474	0.8549	33.5303	33.3143	33.7463	0.0046	0.0040	0.0052
	Textual Tampering - 3	0.8509	0.8472	0.8546	33.4781	33.2484	33.7079	0.0047	0.0041	0.0053
	Graphical Tampering - 1	0.8487	0.8448	0.8527	33.4588	33.2744	33.6431	0.0047	0.0042	0.0052
	Graphical Tampering - 2	0.8487	0.8448	0.8527	33.4588	33.2744	33.6431	0.0047	0.0042	0.0052
	Graphical Tampering - 3	0.8491	0.8451	0.8531	33.4284	33.2341	33.6228	0.0047	0.0042	0.0052
	Painting - 1	0.8513	0.8474	0.8552	33.5253	33.3118	33.7389	0.0048	0.0041	0.0054
	Painting - 2	0.8513	0.8474	0.8552	33.5191	33.3047	33.7335	0.0048	0.0041	0.0054
	Painting - 3	0.8512	0.8473	0.8552	33.5164	33.3019	33.7309	0.0048	0.0042	0.0054
	Textual Tampering - 1	0.8345	0.8298	0.8392	32.0800	31.8087	32.3513	0.0110	0.0101	0.0120
EditGuard	Textual Tampering - 2	0.8340	0.8293	0.8387	32.0741	31.8037	32.3446	0.0111	0.0101	0.0120
	Textual Tampering - 3	0.8337	0.8289	0.8384	32.0629	31.7912	32.3346	0.0111	0.0101	0.0121
	Graphical Tampering - 1	0.8293	0.8245	0.8340	31.6900	31.3810	31.9990	0.0122	0.0110	0.0134
	Graphical Tampering - 2	0.8293	0.8245	0.8340	31.6900	31.3810	31.9990	0.0122	0.0110	0.0134
	Graphical Tampering - 3	0.8299	0.8251	0.8347	31.6523	31.3389	31.9658	0.0123	0.0111	0.0135
	Painting - 1	0.8342	0.8293	0.8391	31.9776	31.6498	32.3055	0.0110	0.0098	0.0122
	Painting - 2	0.8342	0.8293	0.8392	31.9607	31.6314	32.2901	0.0111	0.0098	0.0123
	Painting - 3	0.8345	0.8296	0.8393	31.9600	31.6307	32.2893	0.0111	0.0099	0.0123

## B.2 Accuracy of Tampering Detection

Table 6: The accuracy evaluation results of tampering detection on the AGD. The Mean column represents the average value of each metric (Noise Percentage, RMSE, IoU, F1 Score). The Lower and Upper columns indicate the 95% confidence interval for each metric.

Method	Subset	No Tampering						Post-Tampering					
		Noise Percentage ↓			RMSE ↓			IoU ↑			F1 Score ↑		
		Mean	Lower	Upper	Mean	Lower	Upper	Mean	Lower	Upper	Mean	Lower	Upper
VizDefender	Modifying Data Point Values	0.061%	0.032%	0.090%	0.023	0.016	0.030	0.590	0.445	0.736	0.722	0.593	0.850
	Adding or Removing Data Points	0.103%	0.045%	0.161%	0.030	0.020	0.039	0.771	0.561	0.981	0.834	0.655	1.012
	Modifying Coordinate Values	0.102%	0.028%	0.176%	0.028	0.016	0.039	0.733	0.661	0.804	0.842	0.794	0.890
	Deceptive Auxiliary Annotations	0.090%	0.022%	0.158%	0.026	0.015	0.037	0.562	0.386	0.738	0.693	0.557	0.829
	Modifying Legend	0.064%	0.012%	0.116%	0.023	0.014	0.031	0.763	0.657	0.868	0.858	0.788	0.929
	Hiding Labels	0.083%	0.013%	0.153%	0.024	0.012	0.036	0.779	0.731	0.827	0.874	0.843	0.906
	Adding or Removing Logos	0.021%	0.005%	0.037%	0.012	0.006	0.018	0.906	0.875	0.938	0.950	0.932	0.968
	Data-Visual Disproportion	0.059%	0.045%	0.073%	0.024	0.022	0.027	0.750	0.679	0.820	0.853	0.805	0.901
	Modifying Colormap	0.053%	0.000%	0.136%	0.017	0.005	0.029	0.616	0.473	0.759	0.745	0.635	0.856
	Mixture	0.085%	0.016%	0.154%	0.025	0.013	0.036	0.802	0.729	0.876	0.887	0.839	0.935
EditGuard	Modifying Data Point Values	0.551%	0.398%	0.704%	0.073	0.063	0.083	0.343	0.213	0.473	0.486	0.341	0.631
	Adding or Removing Data Points	0.316%	0.075%	0.557%	0.048	0.026	0.070	0.733	0.506	0.959	0.799	0.595	1.003
	Modifying Coordinate Values	0.534%	0.446%	0.622%	0.073	0.067	0.079	0.481	0.365	0.597	0.635	0.530	0.740
	Deceptive Auxiliary Annotations	0.476%	0.281%	0.671%	0.064	0.045	0.083	0.462	0.260	0.664	0.587	0.400	0.775
	Modifying Legend	0.496%	0.292%	0.700%	0.065	0.045	0.085	0.546	0.367	0.726	0.675	0.519	0.831
	Hiding Labels	0.316%	0.112%	0.520%	0.048	0.027	0.070	0.652	0.510	0.794	0.772	0.655	0.889
	Adding or Removing Logos	0.369%	0.149%	0.589%	0.054	0.032	0.075	0.694	0.524	0.863	0.797	0.671	0.923
	Data-Visual Disproportion	0.646%	0.512%	0.780%	0.080	0.072	0.088	0.444	0.320	0.567	0.596	0.470	0.722
	Modifying Colormap	0.494%	0.250%	0.738%	0.064	0.043	0.086	0.407	0.187	0.627	0.521	0.309	0.733
	Mixture	0.401%	0.117%	0.685%	0.055	0.032	0.079	0.693	0.544	0.842	0.801	0.684	0.918
ManTraNet	Modifying Data Point Values	1.876%	1.373%	2.378%	0.135	0.117	0.153	0.068	0.025	0.112	0.122	0.047	0.197
	Adding or Removing Data Points	2.389%	1.821%	2.958%	0.153	0.134	0.171	0.043	0.000	0.107	0.073	0.000	0.172
	Modifying Coordinate Values	1.887%	1.096%	2.677%	0.133	0.107	0.159	0.001	0.000	0.002	0.002	0.000	0.004
	Deceptive Auxiliary Annotations	1.508%	0.821%	2.195%	0.117	0.088	0.146	0.180	0.040	0.321	0.269	0.094	0.444
	Modifying Legend	2.716%	1.180%	4.253%	0.157	0.120	0.195	0.008	0.000	0.024	0.016	0.000	0.044
	Hiding Labels	1.627%	1.031%	2.223%	0.123	0.098	0.148	0.018	0.000	0.038	0.035	0.000	0.072
	Adding or Removing Logos	2.563%	1.297%	3.830%	0.152	0.113	0.190	0.069	0.008	0.131	0.120	0.020	0.219
	Data-Visual Disproportion	2.384%	2.010%	2.759%	0.154	0.142	0.166	0.015	0.000	0.037	0.028	0.000	0.068
	Modifying Colormap	3.416%	1.282%	5.550%	0.169	0.112	0.226	0.094	0.000	0.225	0.135	0.000	0.312
	Mixture	3.713%	0.754%	6.671%	0.174	0.112	0.236	0.041	0.000	0.096	0.071	0.000	0.160
MVSS-Net	Modifying Data Point Values	3.220%	0.882%	5.558%	0.154	0.086	0.223	0.010	0.002	0.018	0.031	0.000	0.086
	Adding or Removing Data Points	3.821%	0.953%	6.688%	0.160	0.076	0.245	0.033	0.011	0.055	0.076	0.000	0.177
	Modifying Coordinate Values	4.891%	1.430%	8.352%	0.190	0.106	0.275	0.010	0.004	0.017	0.003	0.000	0.008
	Deceptive Auxiliary Annotations	3.691%	0.873%	6.509%	0.154	0.068	0.241	0.034	0.000	0.072	0.098	0.000	0.226
	Modifying Legend	2.585%	0.322%	4.848%	0.130	0.059	0.201	0.006	0.002	0.011	0.006	0.000	0.015
	Hiding Labels	3.555%	0.000%	7.381%	0.156	0.075	0.236	0.015	0.008	0.022	0.077	0.000	0.162
	Adding or Removing Logos	4.204%	1.687%	6.720%	0.184	0.115	0.252	0.012	0.008	0.016	0.100	0.000	0.230
	Data-Visual Disproportion	3.411%	1.413%	5.410%	0.168	0.110	0.226	0.010	0.003	0.016	0.005	0.000	0.018
	Modifying Colormap	8.136%	2.293%	13.978%	0.237	0.118	0.357	0.031	0.000	0.072	0.014	0.000	0.045
	Mixture	3.859%	1.139%	6.579%	0.169	0.093	0.245	0.022	0.011	0.033	0.051	0.000	0.142

Table 7: The accuracy evaluation results of tampering detection on the MCD. The Mean column represents the average value of each metric (Noise Percentage, RMSE, IoU, F1 Score). The Lower and Upper columns indicate the 95% confidence interval for each metric.

Method	Subset	No Tampering						Post-Tampering					
		Noise Percentage ↓			RMSE ↓			IoU ↑			F1 Score ↑		
		Mean	Lower	Upper	Mean	Lower	Upper	Mean	Lower	Upper	Mean	Lower	Upper
VizDefender	Textual Tampering - 1	0.036%	0.022%	0.049%	0.013	0.010	0.016	0.549	0.494	0.604	0.660	0.604	0.716
	Textual Tampering - 2	0.035%	0.021%	0.048%	0.013	0.010	0.015	0.598	0.553	0.643	0.719	0.677	0.761
	Textual Tampering - 3	0.035%	0.021%	0.048%	0.013	0.010	0.015	0.624	0.583	0.665	0.746	0.709	0.782
	Graphical Tampering - 1	0.034%	0.017%	0.051%	0.011	0.008	0.014	0.552	0.498	0.606	0.665	0.612	0.718
	Graphical Tampering - 2	0.034%	0.017%	0.051%	0.011	0.008	0.014	0.595	0.551	0.639	0.718	0.678	0.759
	Graphical Tampering - 3	0.036%	0.018%	0.053%	0.012	0.009	0.015	0.606	0.563	0.649	0.729	0.690	0.767
	Painting - 1	0.049%	0.025%	0.073%	0.014	0.011	0.018	0.290	0.261	0.319	0.430	0.395	0.465
	Painting - 2	0.049%	0.025%	0.073%	0.014	0.011	0.018	0.294	0.269	0.319	0.439	0.409	0.470
	Painting - 3	0.049%	0.025%	0.073%	0.014	0.011	0.018	0.303	0.279	0.326	0.452	0.424	0.480
EditGuard	Textual Tampering - 1	0.635%	0.574%	0.697%	0.076	0.072	0.081	0.120	0.093	0.147	0.193	0.157	0.228
	Textual Tampering - 2	0.622%	0.561%	0.684%	0.075	0.071	0.080	0.195	0.159	0.231	0.295	0.253	0.337
	Textual Tampering - 3	0.625%	0.563%	0.687%	0.076	0.071	0.080	0.246	0.209	0.282	0.363	0.320	0.406
	Graphical Tampering - 1	0.577%	0.517%	0.637%	0.072	0.067	0.077	0.294	0.248	0.340	0.407	0.352	0.461
	Graphical Tampering - 2	0.577%	0.517%	0.637%	0.072	0.067	0.077	0.388	0.340	0.435	0.513	0.460	0.567
	Graphical Tampering - 3	0.585%	0.524%	0.647%	0.073	0.068	0.077	0.431	0.382	0.479	0.557	0.504	0.610
	Painting - 1	0.614%	0.553%	0.675%	0.075	0.070	0.079	0.117	0.095	0.138	0.194	0.163	0.225
	Painting - 2	0.617%	0.555%	0.678%	0.075	0.070	0.080	0.147	0.125	0.169	0.241	0.210	0.272
	Painting - 3	0.616%	0.554%	0.677%	0.075	0.070	0.079	0.177	0.156	0.199	0.288	0.258	0.317
ManTraNet	Textual Tampering - 1	4.256%	3.537%	4.976%	0.191	0.176	0.207	0.001	0.000	0.001	0.001	0.000	0.002
	Textual Tampering - 2	4.194%	3.474%	4.915%	0.190	0.174	0.205	0.001	0.000	0.002	0.003	0.000	0.005
	Textual Tampering - 3	4.225%	3.508%	4.943%	0.191	0.175	0.206	0.003	0.001	0.006	0.006	0.001	0.010
	Graphical Tampering - 1	4.168%	3.519%	4.817%	0.190	0.176	0.205	0.017	0.012	0.022	0.033	0.024	0.042
	Graphical Tampering - 2	4.168%	3.519%	4.817%	0.190	0.176	0.205	0.043	0.032	0.054	0.077	0.059	0.095
	Graphical Tampering - 3	4.170%	3.521%	4.819%	0.190	0.176	0.205	0.056	0.042	0.070	0.099	0.078	0.120
	Painting - 1	5.140%	4.155%	6.125%	0.206	0.188	0.225	0.042	0.030	0.054	0.075	0.056	0.095
	Painting - 2	5.127%	4.144%	6.111%	0.206	0.187	0.225	0.072	0.052	0.092	0.121	0.092	0.150
	Painting - 3	5.126%	4.142%	6.110%	0.206	0.187	0.225	0.097	0.074	0.119	0.159	0.126	0.192
MVSS-Net	Textual Tampering - 1	4.275%	2.870%	5.681%	0.142	0.111	0.172	0.001	0.001	0.001	0.001	0.000	0.002
	Textual Tampering - 2	4.206%	2.799%	5.614%	0.139	0.109	0.169	0.002	0.001	0.004	0.002	0.000	0.004
	Textual Tampering - 3	4.206%	2.799%	5.614%	0.139	0.109	0.169	0.003	0.001	0.005	0.002	0.000	0.005
	Graphical Tampering - 1	4.448%	3.178%	5.718%	0.156	0.128	0.184	0.006	0.004	0.007	0.064	0.038	0.091
	Graphical Tampering - 2	4.448%	3.178%	5.718%	0.156	0.128	0.184	0.012	0.009	0.014	0.121	0.083	0.160
	Graphical Tampering - 3	4.520%	3.252%	5.789%	0.159	0.130	0.187	0.017	0.014	0.021	0.164	0.126	0.202
	Painting - 1	4.378%	2.793%	5.963%	0.147	0.117	0.177	0.002	0.001	0.002	0.070	0.043	0.096
	Painting - 2	4.438%	2.855%	6.021%	0.149	0.120	0.179	0.005	0.002	0.008	0.074	0.053	0.094
	Painting - 3	4.438%	2.855%	6.021%	0.149	0.120	0.179	0.007	0.005	0.008	0.084	0.062	0.106

### B.3 Accuracy of Intent Analysis

Table 8: The accuracy evaluation results of tampering intent analysis on the MCD. The Mean column represents the average value of each metric (Cosine Similarity of Tampering Method and Tampering Intent). The Lower and Upper columns indicate the 95% confidence interval for each metric.

Method	Tampering Type	Tampering Process Similarity			Tampering Intent Similarity		
		Mean	Lower	Upper	Mean	Lower	Upper
VizDefender	Modifying Data Point Values	0.8569	0.8266	0.8873	0.9021	0.8749	0.9292
	Adding or Removing Data Points	0.8751	0.8466	0.9037	0.9000	0.8850	0.9151
	Modifying Coordinate Values	0.8590	0.8310	0.8871	0.9133	0.8972	0.9295
	Deceptive Auxiliary Annotations	0.8609	0.8449	0.8770	0.8950	0.8730	0.9169
	Modifying Legend	0.8760	0.8557	0.8962	0.9017	0.8808	0.9225
	Hiding Labels	0.9077	0.8770	0.9384	0.9320	0.9132	0.9507
	Adding or Removing Logos	0.8732	0.8495	0.8970	0.9145	0.8958	0.9333
	Data-Visual Disproportion	0.8815	0.8608	0.9022	0.9040	0.8816	0.9264
	Modifying Colormap	0.8443	0.8206	0.8681	0.8933	0.8739	0.9126
	Mixture	0.9063	0.8922	0.9203	0.9162	0.8942	0.9381
Baseline	Modifying Data Point Values	0.8407	0.8208	0.8605	0.8983	0.8743	0.9223
	Adding or Removing Data Points	0.8243	0.7863	0.8622	0.8546	0.8277	0.8815
	Modifying Coordinate Values	0.8283	0.7954	0.8611	0.8670	0.8409	0.8931
	Deceptive Auxiliary Annotations	0.8600	0.8438	0.8762	0.8998	0.8860	0.9136
	Modifying Legend	0.8592	0.8398	0.8787	0.8802	0.8565	0.9040
	Hiding Labels	0.8353	0.8091	0.8614	0.8914	0.8638	0.9191
	Adding or Removing Logos	0.7897	0.7555	0.8240	0.8692	0.8422	0.8961
	Data-Visual Disproportion	0.8643	0.8423	0.8863	0.8886	0.8627	0.9145
	Modifying Colormap	0.8375	0.8066	0.8684	0.8797	0.8655	0.8939
	Mixture	0.8189	0.8031	0.8346	0.8820	0.8694	0.8945

### C VISUAL COMPARISON

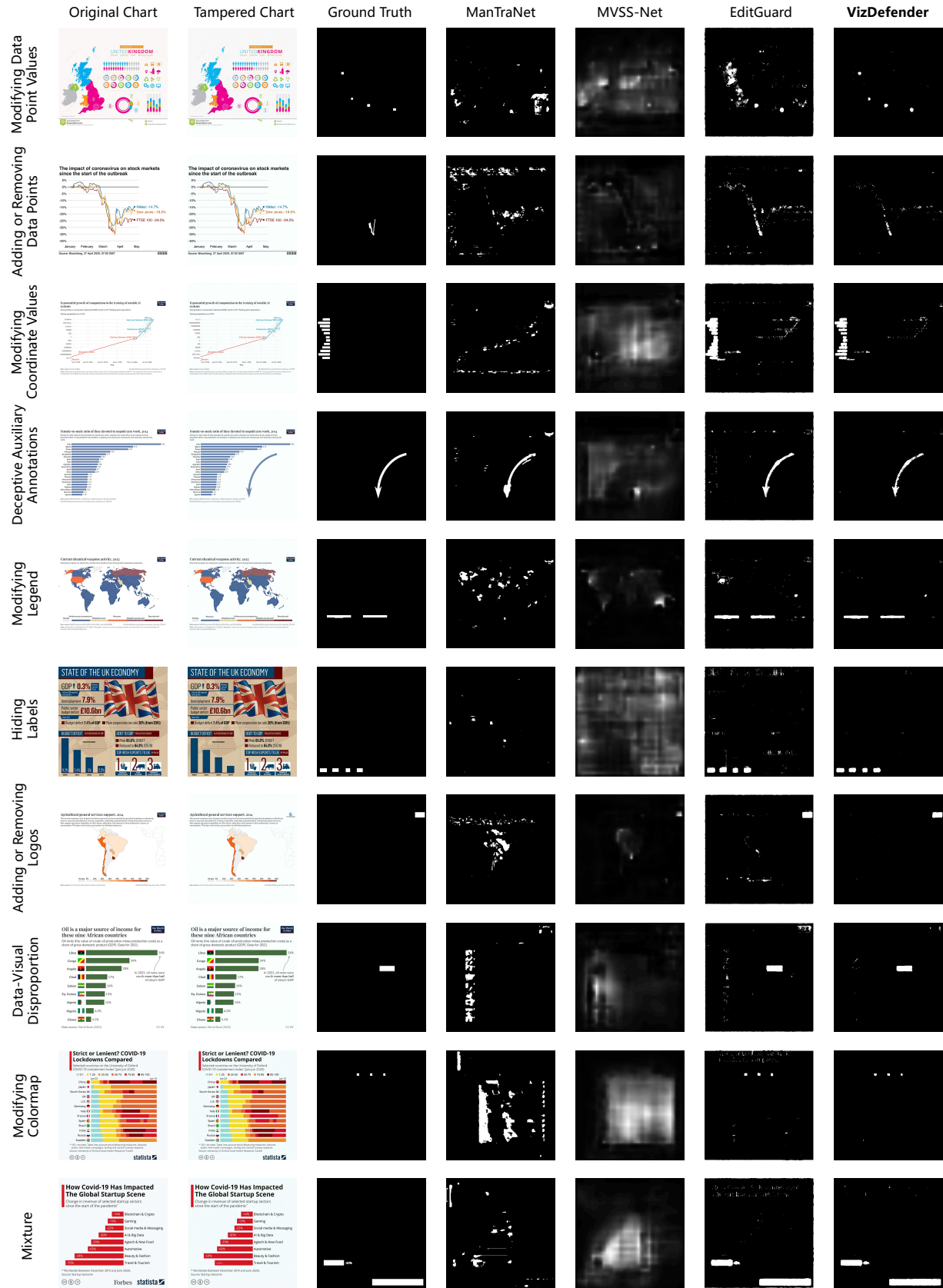


Fig. 14: Visual comparison of tampering detection on the MCD.

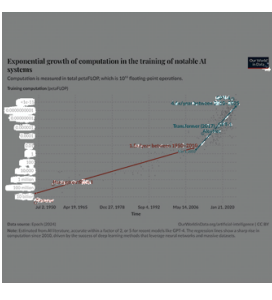
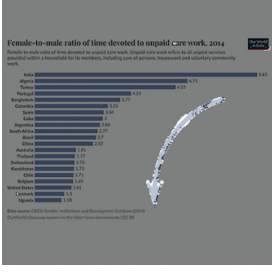
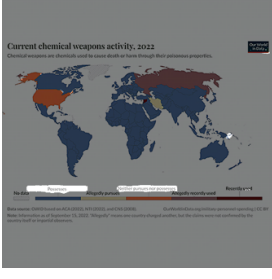
Detection Mask	Ground Truth	w/o Agent Design	Ours
	<p><b>Ground Truth</b></p> <p><b>Tampering Method:</b> Modifying data point values</p> <p><b>Tampering Process:</b> Increase the population value of England from 53 million to 60 million and decrease the population value of Scotland from 5.2 million to 4 million.</p> <p><b>Intent:</b> To manipulate the perception of population distribution, making England appear more populous and Scotland less populous, potentially influencing political or economic decisions based on population size.</p>	<p><b>Tampering Method:</b> Data-visual disproportion</p> <p><b>Tampering Process:</b> The text elements indicating population numbers for Scotland (4) and returns (50%) for Wales in the chart have been altered. Specifically, the numbers were blurred or obscured to make them unreadable or less clear.</p> <p><b>Intent:</b> The intent behind the tampering could be to mislead viewers or readers about the accurate population statistics of the regions or to modify perceived performance metrics associated with these regions in a potentially sensitive or competitive context. This could influence opinions, decisions, or narratives associated with the viewer's understanding of demographic distribution across the United Kingdom.</p>	<p><b>Tampering Method:</b> Modifying data point values</p> <p><b>Tampering Process:</b> Increase the population value of England and decrease the population value of Scotland.</p> <p><b>Intent:</b> The purpose of increasing England's population while decreasing Scotland's is to alter perceptions of population distribution, potentially to support a narrative about demographic trends or resource allocation.</p>
	<p><b>Ground Truth</b></p> <p><b>Tampering Method:</b> Adding or Removing Data Points</p> <p><b>Tampering Process:</b> Removing the data point for Rockbank - Mount Cottrell (59.4%)</p> <p><b>Intent:</b> To make Mickleham - Yuroke appear as the fastest-growing city in Australia, thereby altering the perceived growth trend.</p>	<p><b>Tampering Method:</b> Modifying data point values</p> <p><b>Tampering Process:</b> The bar for 'Mickleham - Yuroke' has been extended significantly, and its value has been increased from an original value (likely around 25-30%) to 52.2%.</p> <p><b>Intent:</b> To exaggerate the growth of 'Mickleham - Yuroke' by showing a much larger percentage than its actual value, potentially to highlight its status as the fastest-growing city with an even greater margin.</p>	<p><b>Tampering Method:</b> Adding or Removing Data Points</p> <p><b>Tampering Process:</b> Remove the data point representing the top-ranked city, including its city name, growth percentage, and associated bar, from the list.</p> <p><b>Intent:</b> To conceal the identity and growth rate of the actual fastest-growing city, thereby misrepresenting the true rankings of urban growth in Australia.</p>
	<p><b>Ground Truth</b></p> <p><b>Tampering Method:</b> Modifying coordinate values</p> <p><b>Tampering Process:</b> Reverse the Y-axis so that the exponential growth trend appears as an exponential decline.</p> <p><b>Intent:</b> To mislead viewers into thinking that the computational growth in AI systems has been decreasing over time, rather than increasing.</p>	<p><b>Tampering Method:</b> Modifying data point values</p> <p><b>Tampering Process:</b> Blurring and data obscuration.</p> <p><b>Intent:</b> The blurring of sections of the chart including the x-axis dates and y-axis values in the tampering detection mask suggests an intent to obscure specific data points and trends in AI computation growth. This could be to prevent accurate interpretation of the chart's data regarding the exponential growth speed and milestones of AI development, possibly to manipulate understanding or insights into this trend among viewers.</p>	<p><b>Tampering Method:</b> Modifying coordinate values</p> <p><b>Tampering Process:</b> The computational values along the y-axis were modified, likely inflating original values to make certain trends appear more exponential and significant.</p> <p><b>Intent:</b> The purpose of altering these values is to exaggerate the growth rates of computational power over the years, possibly to suggest a more rapid or slower technological advancement in AI systems.</p>
	<p><b>Ground Truth</b></p> <p><b>Tampering Method:</b> Deceptive Annotations</p> <p><b>Tampering Process:</b> Adding a directional arrow to the chart to suggest a decreasing trend in the female-to-male ratio of time devoted to unpaid care work.</p> <p><b>Intent:</b> To create a false impression that the gender disparity in unpaid care work is decreasing over these countries, potentially to support a biased argument that gender equality is improving in this area.</p>	<p><b>Tampering Method:</b> Deceptive Annotations</p> <p><b>Tampering Process:</b> Adding a misleading arrow to suggest a relationship or involvement not supported by data.</p> <p><b>Intent:</b> The purpose of the arrow is to create a false impression that there is a significant or notable relationship or trend indicated by the arrow, potentially drawing attention away from the actual data presented.</p>	<p><b>Tampering Method:</b> Deceptive Annotations</p> <p><b>Tampering Process:</b> An arrow was added to the chart pointing at Uganda, which had a markedly lower female-to-male ratio of time devoted to unpaid care work compared to India.</p> <p><b>Intent:</b> The intent behind the tampering might have been to draw attention to Uganda's data point, highlighting its lower ratio in unpaid care work in contrast to other countries like India. This could suggest a focus on particular data that may align with a specific narrative or agenda, possibly implying progress or a more balanced unpaid care burden in Uganda.</p>
	<p><b>Ground Truth</b></p> <p><b>Tampering Method:</b> Modifying the legend</p> <p><b>Tampering Process:</b> Swapping the 'Possesses' and 'Neither pursues nor possesses' labels in the legend.</p> <p><b>Intent:</b> To mislead viewers into thinking that countries that do not possess chemical weapons actually do, and vice versa, potentially altering the perception of global chemical weapon threats.</p>	<p><b>Tampering Method:</b> Modifying the legend</p> <p><b>Tampering Process:</b> The tampering process involved modifying the map by altering the legend's description for the extent of possession of chemical weapons. The label 'Neither pursues nor possesses' has been changed to spread a misleading categorization of countries.</p> <p><b>Intent:</b> The intent behind this tampering seems to be an attempt to manipulate public perception or political narratives regarding the involvement of specific countries in chemical weapons activities by changing the legend that could potentially alter how the data is interpreted without a proper understanding of the tampering.</p>	<p><b>Tampering Method:</b> Modifying the legend</p> <p><b>Tampering Process:</b> Change the color coding of the legend for 'Possesses' and 'Neither pursues nor possesses' to mislead viewers about which countries are involved with chemical weapons.</p> <p><b>Intent:</b> The purpose of this tampering is to mislead viewers by suggesting that specific countries possess chemical weapons or are neutral, which could skew reader perceptions and interpretations of geopolitical stances on chemical weapon policies.</p>

Fig. 15: Visual comparison of intent analysis on the AGD (the first five subsets).

Detection Mask	Ground Truth	w/o Agent Design	Ours
	<p><b>Ground Truth</b></p> <p><b>Tampering Method:</b> Hiding labels</p> <p><b>Tampering Process:</b> Remove the numerical values next to the bars indicating the mean download speed in Megabits per second (in Mbps)</p> <p><b>Intent:</b> To obscure the actual download speeds and make it difficult for viewers to compare the internet speeds of different countries accurately.</p>	<p><b>Tampering Method:</b> Modifying data point values</p> <p><b>Tampering Process:</b> The lengths of the horizontal bars have been extended to exaggerate the data values, making the countries appear to have faster internet speeds than they actually do.</p> <p><b>Intent:</b> To mislead viewers into believing that the listed countries have significantly faster internet speeds, potentially for promotional purposes or to make a political statement about internet infrastructure.</p>	<p><b>Tampering Method:</b> Hiding labels</p> <p><b>Tampering Process:</b> The numerical data labels, which would specify the mean download speed for each country, have been hidden or removed from the ends of the bars.</p> <p><b>Intent:</b> To prevent precise comparison of download speeds between countries, making it harder for viewers to scrutinize exact performance metrics and forcing them to rely solely on the visual length of the bars.</p>
	<p><b>Tampering Method:</b> Adding or removing logos</p> <p><b>Tampering Process:</b> Remove the 'Our World in Data' logo and replace it with a different logo, such as 'Nvidia'.</p> <p><b>Intent:</b> To mislead viewers about the data source, making them believe the data is provided by 'Nvidia' instead of 'Our World in Data'.</p>	<p><b>Tampering Method:</b> Modifying the legend</p> <p><b>Tampering Process:</b> The legend has been altered to misrepresent the 'AMD' manufacturer with a blue square, but the corresponding data point 'AMD Radeon RX 7900 XTX' is colored green, indicating it is incorrectly associated with 'NVIDIA'.</p> <p><b>Intent:</b> To deceptively attribute a high-performing AMD product to NVIDIA, thus making NVIDIA's performance appear superior or more dominant than it actually is.</p>	<p><b>Tampering Method:</b> Adding or removing logos</p> <p><b>Tampering Process:</b> The NVIDIA logo was added to the top-right corner of the chart.</p> <p><b>Intent:</b> To capitalize NVIDIA's brand and imply the chart's findings are directly associated with or endorsed by the company, leveraging its prominent placement to influence viewer perception.</p>
	<p><b>Tampering Method:</b> Data-visual Disproportion</p> <p><b>Tampering Process:</b> Decreased the size of the green section representing migration from Asia.</p> <p><b>Intent:</b> To make migration from Asia appear less significant, misleading viewers about its importance in global migration.</p>	<p><b>Tampering Method:</b> Modifying data point values</p> <p><b>Tampering Process:</b> The bar representing 'Asia 115M' on the left side has been visually extended to be significantly longer than its corresponding numerical value would suggest, creating a disproportionately large visual representation.</p> <p><b>Intent:</b> To exaggerate the number of migrants originating from Asia by making its bar appear much larger than it actually is, potentially to highlight or overemphasize Asia's role in international migration.</p>	<p><b>Tampering Method:</b> Data-visual Disproportion</p> <p><b>Tampering Process:</b> The visual width of the 'Asia' destination bar (81M) has been inflated to appear similar in size to the 'Asia' source bar (115M), despite representing a smaller value.</p> <p><b>Intent:</b> To visually downplay the proportion of international migrants who move to Asia, creating a misleading impression that Asia receives a much smaller share of migrants than its actual data value suggests relative to its source migrants.</p>
	<p><b>Tampering Method:</b> Modifying the colormap</p> <p><b>Tampering Process:</b> Disrupt the color mapping for the ranges 25-50, 50-75, and 75-100.</p> <p><b>Intent:</b> The intention behind this alteration is to confuse the interpretation of lockdown strictness by misrepresenting the data visually. By switching colors between similar values, it may lead viewers to misunderstand the levels of restrictions imposed by different countries, potentially affecting public perception and discussions regarding the effectiveness of lockdown measures.</p>	<p><b>Tampering Method:</b> Modifying data point values</p> <p><b>Tampering Process:</b> The lengths of the colored segments within the horizontal bars have been altered, specifically making the '75-85' and '85-100' categories appear longer for most countries, while shrinking the '0-1' and '1-25' categories.</p> <p><b>Intent:</b> The intent is to exaggerate the strictness of COVID-19 lockdowns, making it seem as though countries implemented stricter measures for longer durations than they actually did.</p>	<p><b>Tampering Method:</b> Modifying the colormap</p> <p><b>Tampering Process:</b> Altered the color values in the legend for categories 25-50, 50-75, and 75-85.</p> <p><b>Intent:</b> To distort the perception of the strictness levels of COVID-19 lockdowns by misrepresenting the color scheme that indicates different levels.</p>
	<p><b>Tampering Method:</b> Adding or Removing Data Points; Adding or Removing logos</p> <p><b>Tampering Process:</b> Remove data for Netherlands and Norway, remove the logo from the bottom right corner.</p> <p><b>Intent:</b> The purpose of this modification is to omit specific data points that might offer a more comprehensive view of the situation, potentially skewing perceptions of the impact on mental health by focusing on countries with higher percentages. This could lead to a biased interpretation of the data, influencing public perception or policy discussions based on incomplete information.</p>	<p><b>Tampering Method:</b> Data-visual disproportion; Hiding Labels</p> <p><b>Tampering Process:</b> The lengths of the bars do not accurately correspond to their numerical values; for instance, the bar for 18% appears disproportionately long compared to 33%, and the bars for 26% and 24% also seem visually distorted. Portions of the text and potentially other elements (like logos or disclaimers) are obscured or removed by solid white rectangles.</p> <p><b>Intent:</b> To visually manipulate the perceived differences between data points, making smaller values appear relatively larger or larger values appear relatively smaller than they are, thus influencing the viewer's interpretation without altering the numerical labels.</p>	<p><b>Tampering Method:</b> Adding or Removing Data Points; Adding or Removing logos</p> <p><b>Tampering Process:</b> Removed additional data points, including country names, flags, bars, and their corresponding percentages, that were originally present below Sweden; Removed a logo or branding element from the bottom right corner of the chart.</p> <p><b>Intent:</b> To selectively remove data points, potentially to hide information about other countries' mental health impact or to manipulate the perceived ranking or comparison of the displayed countries.</p>

Fig. 16: Visual comparison of intent analysis on the AGD (the second five subsets).

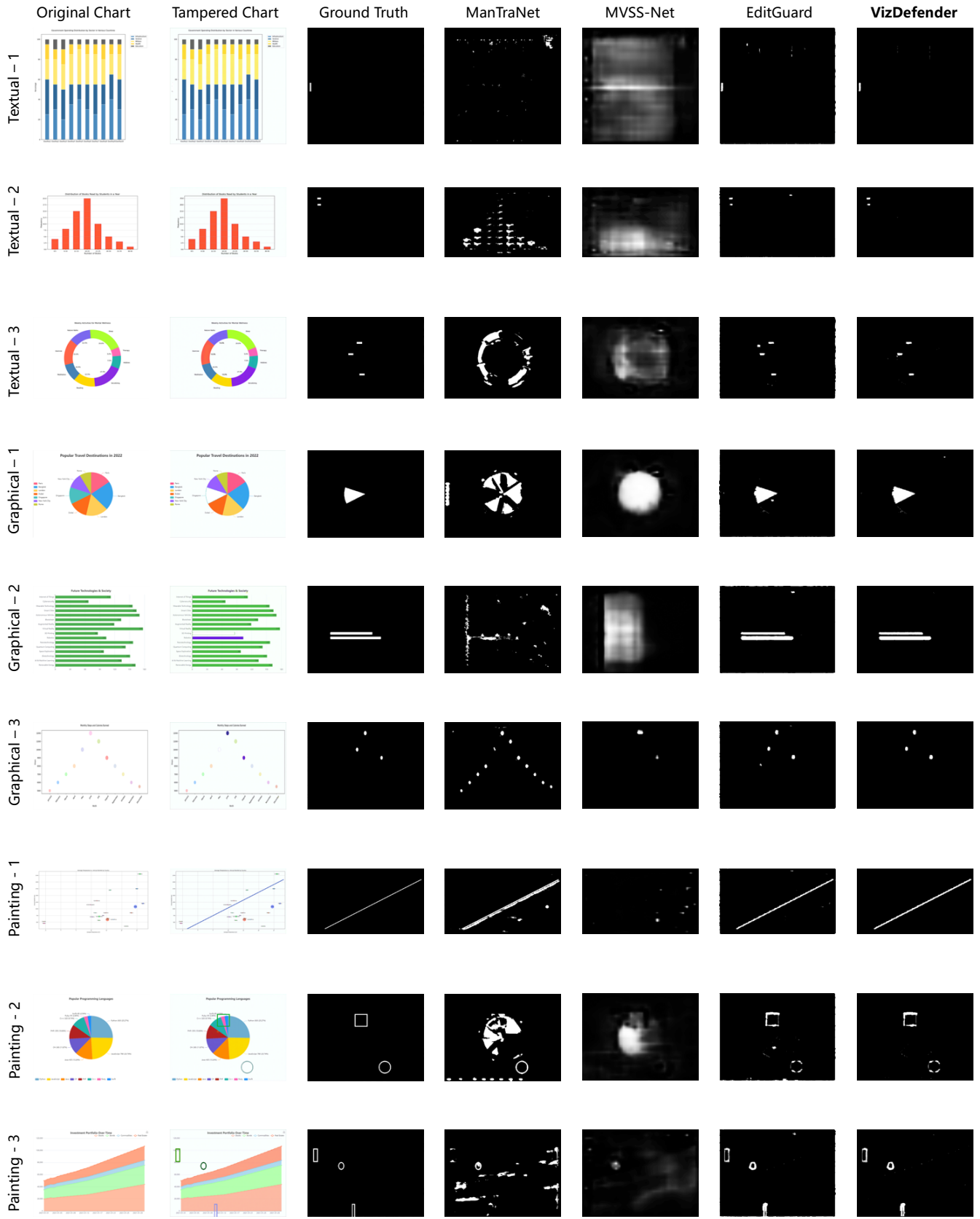


Fig. 17: Visual comparison of tampering detection on the AGD.

## D FAILURE ANALYSIS

### D.1 Tampering Detection

The current tampering detection method in the VizDefender system still faces certain failure cases. By analyzing two primary errors, we find that these issues collectively highlight the model's insufficient sensitivity to fine details, particularly in thin-line structures. Most of these noise artifacts can be effectively addressed through our Mask Refinement Agent.

**Noise in Text Region Detection.** As shown in Fig. 18, in the process of detecting tampering in text regions, the model often generates extraneous noise responses at the edges of characters. This results in false-positive outputs that resemble burr-like anomalies, which degrade the accuracy of detecting true tampered regions. These artifacts can lead to misjudgments, especially in cases where the tampered regions are subtle or where the noise is incorrectly identified as tampering.

The error may stem from the fact that visualization images, in contrast to natural images, often include large areas of blank space with high brightness. During the watermarking process, we used DWT, which primarily targets embedding watermarks in high-frequency regions. For visualizations with large blank areas, the high-frequency components are concentrated in the text regions. Since the amount of watermarked information is fixed, the watermark is prone to damage during file transmission, leading to noise appearing more frequently in text regions.

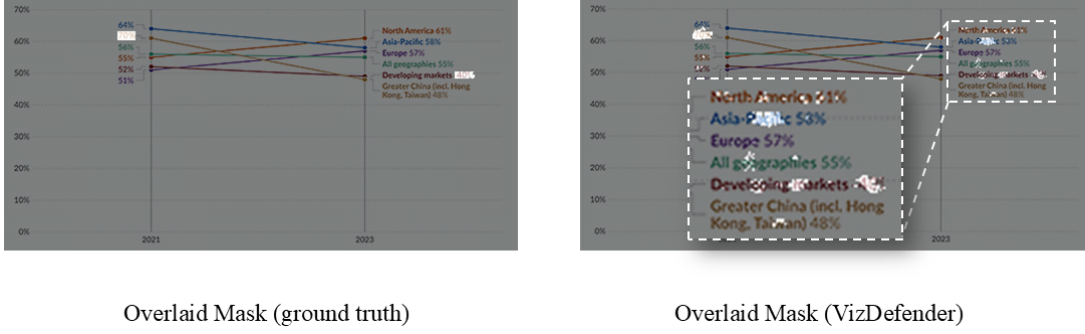


Fig. 18: Error map of Noise in Text Region Detection. The rectangular boxes in the figure represent the locations where errors occur.

**False Detection of Thin-Line Structures.** As shown in Fig. 19, for images containing thin-line structures, such as lines in line charts, the model tends to produce noise along the lines themselves. These noise artifacts are frequently mistaken for genuine tampering traces, such as erasures or additions of lines. As a result, the system's ability to discern between natural features and tampered areas is compromised, leading to incorrect detection of tampering in the absence of such changes.

The error may occur due to thin lines being vulnerable to information loss during the convolution process. During the deconvolution process, these fine details are often further degraded, leading to the loss of critical information and resulting in noise artifacts along the lines.

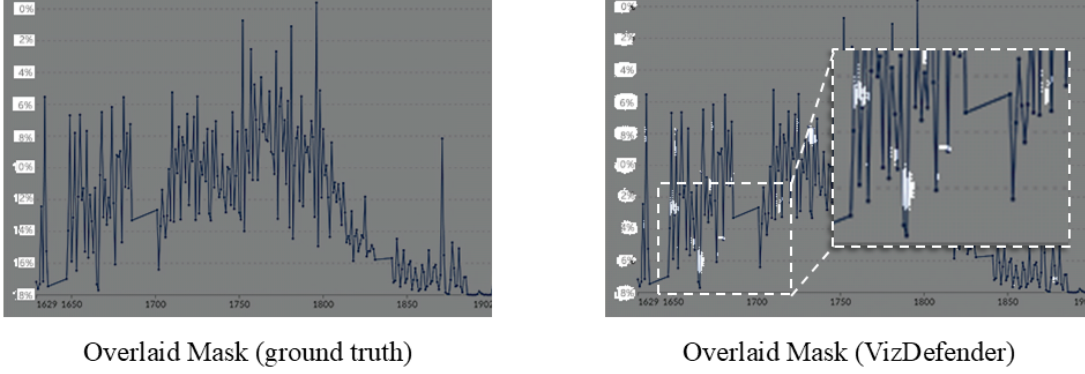


Fig. 19: Error map of False Detection of Thin-Line Structures. The rectangular boxes in the figure represent the locations where errors occur.

## D.2 Tampering Method and Intent Analysis Inference

The current tampering method and intent analysis inference in the VizDefender system faces challenges when tampering involves domain-specific references or context. The agent has difficulty leveraging prior knowledge to infer tampering method or intent because of the lack of the original visualization. As shown in Fig. 20, when tampering involves specific locations, such as “*Marion Correctional Institution with 2,439 cases*”, the agent lacks the information of this target. This absence of prior knowledge results in the model incorrectly predicting the tampering intent as simply obscuring the lower section of the visualization to hide data, instead of recognizing the true manipulation, which involves removing the data for Marion Correctional Institution. Consequently, the model misinterprets both the tampering method and intent, failing to accurately identify the underlying manipulation.

This limitation is not only an issue for VizDefender but also for human judgment. In cases where individuals lack the necessary domain knowledge or context, similar misinterpretations can occur. Therefore, a potential solution for future work is to leverage the prior visualization information into the images.

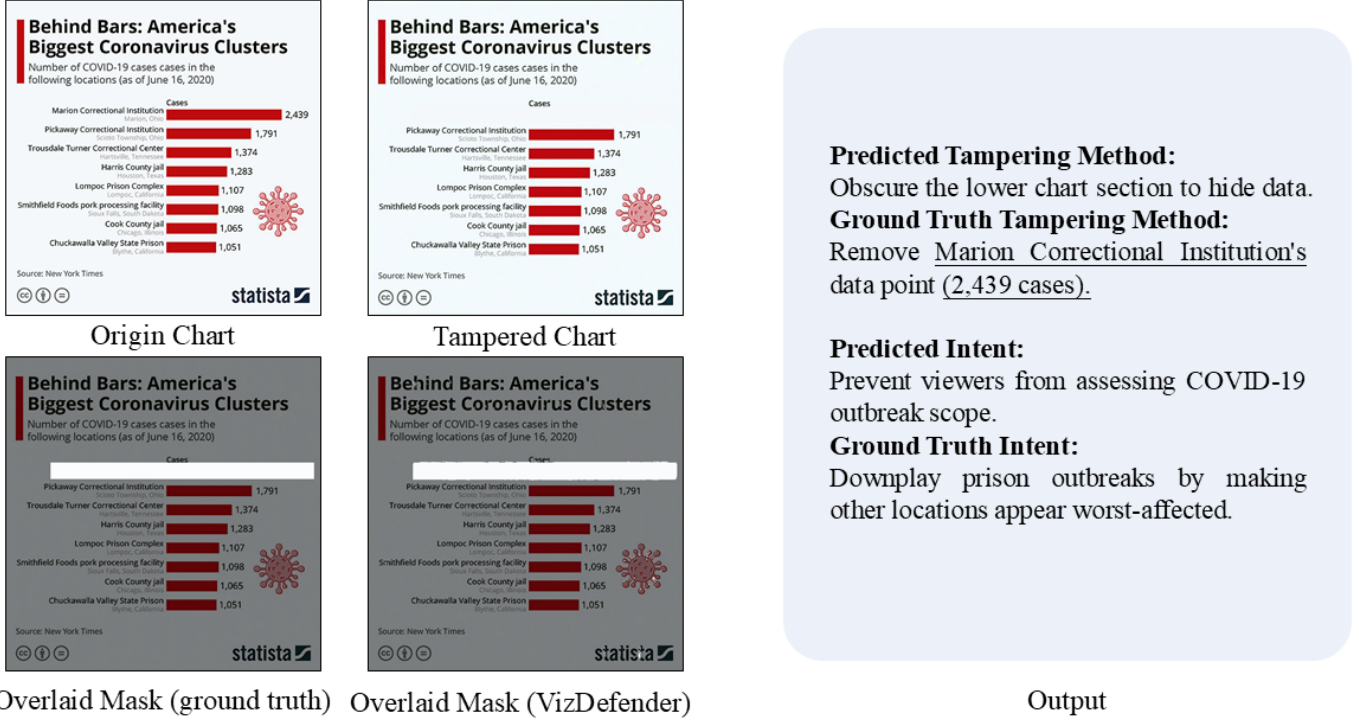


Fig. 20: Illustration of tampering intent inference when prior knowledge is absent. The horizontal line in the tampered visualization represents the lack of prior knowledge about the removed data point, leading to the model misinterpreting the tampering method and intent.